RESEARCH DIVISION
COLLEGE OF ENGINEERING
NEW YORK UNIVERSITY
DEPARTMENT OF METEOROLOGY

A UNIFIED MATHEMATICAL THEORY FOR THE ANALYSIS, PROPAGATION, AND REFRACTION OF STORM GENERATED OCEAN SURFACE WAVES

PART II

Prepared for
BEACH EROSION BOARD DEPARTMENT OF THE ARMY
Contract No. W 49-055-eng-1
OFFICE OF NAVAL RESEARCH DEPARTMENT OF THE NAVY
Contract No. N onr-285(03)

analysis, propogation,
in surface waves. Part

f Engineering, Department of Meteo

	Returned
- x2871	30 Oct 88

A UNIFIED MATHEMATICAL THEORY FOR THE ANALYSIS, PROPAGATION, AND REFRACTION OF STORM GENERATED OCEAN SURFACE WAVES

Part II

By

Willard J. Pierson, Jr.

Preliminary distribution

Prepared under contracts sponsored by the Office of Naval Research and the Beach Erosion Board, Washington, D. C.

New York University
College of Engineering
Department of Meteorology

July 1, 1952

Preface

The following pages represent part two of a book entitled "A Unified Mathematical Theory for the Analysis, Propagation, and Refraction of Storm Generated Ocean Surface Waves." They contain three chapters which logically follow part one as presented in March 1952. Chapters 11 and 12 complete the mathematical derivations to be presented by giving additional properties of waves in deep water and by deriving the procedures for the analysis of pressure and wave records in waters of finite depth and for the refraction of a short crested Gaussian sea surface.

Chapter 13 is the beginning of that part of the book which deals with the practical application of the theories presented in the previous twelve chapters. It treats specific examples of wave and pressure record analysis both by numerical and electronic methods.

Part three is still in preparation, and upon its publication, this book will be complete. There will be two more chapters. One chapter will deal with observations which confirm the forecasting theory; and in it a hypothetically complete forecast will be carried out. The last chapter will comment on current wave generation theory and on the scope of the task which still needs to be done in order to put these theoretical results on a firm practical basis. Part three may be somewhat delayed because of a summer vacation for the author.

July 1, 1952

Willard J. Pierson, Jr.
Department of Meteorology
New York University

Index to Part II

CHAPTER 11

ADDITIONAL PROPERTIES OF A SHORT CRESTED GAUSSIAN SEA SURFACE IN INFINITELY DEEP WATER

Introduction

In this chapter, the pressure, velocity fields and curvature of the short crested sea surface will be studied. In addition, some of the very important lines of future research which are possible by the use of these new concepts will be suggested. Once $[A_2(\mu,\theta)]^2$ has been determined, all of the other desired properties of the sea surface and the fluid motions can be determined to within the accuracy of the linearization assumptions at the start of Chapter 2. Since the sea surface is Gaussian, it follows that all of the other properties of the wave motion such as the fluid velocities, the pressure, and the slope and curvature of the sea surface will be Gaussian. The functions which describe the range of variability of these properties are different from those which describe the sea surface. They are various integrals and functional modifications involving the power spectrum of the free surface which lead to some very important results about the nature of the power spectrum.

Pressure

In Chapter 4, equations (4.8) and (4.10) presented formulas for the pressure at a point below the surface produced by a finite wave group passing overhead. They are considered here only to show how complex the problem can become when an attempt to solve it by Fourier Integral Theory is made. Equation (4.10) shows that at x equal to zero the period of the waves recorded by a sub-surface

Additional Properties of a Short Crested Gaussian Sea Surface in Infinitely Deep Water

$$\eta(x,y,t) = \int_0^{\infty}\int_{-\frac{\pi}{2}}^{\frac{\pi}{2}} \cos\left(\frac{\mu^2}{g}(x\cos\theta + y\sin\theta) - \mu t + \psi(\mu,\theta)\right)\sqrt{[A_2(\mu,\theta)]^2 d\theta d\mu}$$

$$= \lim_{\substack{\Delta_1\mu\to 0\\ \Delta_1\theta\to 0}} \sum_{n=0}^{R-1}\sum_{p=0}^{S-1} \cos\left[\frac{(\mu_{2n+1})^2}{g}(x\cos\theta_{2p+1} + y\sin\theta_{2p+1}) - \mu_{2n+1}t + \psi(\mu_{2n+1},\theta_{2p+1})\right]\sqrt{\left[A_2(\mu_{(2n+1)},\theta_{(2n+1)})\right]^2(\mu_{2n+2}-\mu_{2n})(\theta_{2p+2}-\theta_{2p})} \tag{11.1}$$

$$\mu_{2R}\to+\infty,\quad \theta_{2s}-\frac{\pi}{2}\to 0^+$$

$$P(x,y,t) = \lim_{\substack{\Delta_1\mu\to 0\\ \Delta_1\theta\to 0}} \rho g \sum_{n=0}^{R-1}\sum_{p=0}^{S-1} \cos\left[\frac{(\mu_{2n+1})^2}{g}(x\cos\theta_{2p+1} + y\sin\theta_{2p+1}) - \mu_{2n+1}t + \psi(\mu_{2n+1},\theta_{2p+1})\right] e^{(\mu_{2n+1})^2 z/g}$$
$$\cdot\sqrt{[A_2(\mu_{2n+1},\theta_{2p+1})]^2(\mu_{2n+2}-\mu_{2n})(\theta_{p+2}-\theta_{2p})} - g\rho z$$

$$\mu_{2R}\to+\infty,\quad \theta_{2s}-\frac{\pi}{2}\to 0^+$$

$$= \rho g\int_0^{\infty}\int_{-\frac{\pi}{2}}^{\frac{\pi}{2}} \cos\left(\frac{\mu^2}{g}(x\cos\theta + y\sin\theta) - \mu t + \psi(\mu,\theta)\right)\sqrt{e^{2\mu^2 z/g}\,[A_2(\mu,\theta)]^2 d\theta d\mu} - g\rho z \tag{11.2}$$

$$P_0(t,z) = \rho g\int_0^{\infty} \cos(\mu t + \psi(\mu))\sqrt{e^{2\mu^2 z/g}\,[A(\mu)^2]^2 d\mu} = \rho g\int_0^{\infty} \cos\left[\mu t + \psi(\mu)\right]\sqrt{dE_p(\mu)} \tag{11.3}$$

$$\left[A_p(\mu)\right]^2 = e^{2\mu^2 z/g}\left[A(\mu)\right]^2 \tag{11.4}$$

$$E_p(\mu) = \int_0^{\mu}\left[A_p(\mu^*)\right]^2 d\mu^* \tag{11.5}$$

$$E_{p\max} = \int_0^{\infty} e^{2\mu^{*2} z/g}\left[A(\mu^*)\right]^2 d\mu^* \tag{11.6}$$

pressure recorder becomes larger and larger with increasing depth. In fact a little investigation shows that there will be crests observed in the pressure at the depth, z = -h, when an actual trough of the sea surface is passing overhead. Additional investigation of these formulas will be left to the reader.

The pressure recorded at a depth, z, below the sea surface (z is negative) can be found from the following arguments. The free surface is given by equation (11.1), and it can also be represented by the limit of a partial sum as in the second expression in equation (11.1). For each term in the partial sum, the pressure contribution to the total pressure for that partial sum is found by simply inserting $\rho g \exp((\mu_{2n+1})^2 z/g)$ for each cosine term in equation (11.2). A term for the static pressure is also needed.

The limiting form is then given by the Gaussian Lebesgue Power Integral in the second expression in equation (11.2). The pressure at each point below the sea surface thus involves the contribution of each of the elemental waves passing overhead modified by the appropriate damping effect with depth.

Pressure is usually only recorded at one fixed point. From the results of the first part of Chapter 10, the pressure at the point, x_1, y_1, at any fixed depth, z, is given by equation (11.3). Thus the pressure as a function of time alone is Gaussian. A given pressure record can be analyzed for its power spectrum in the same way that a wave record of the sea surface can be analyzed for its power spectrum. The pressure power spectrum, $[A_p(\mu)]^2$, is related to the power spectrum for the free surface, $[A(\mu)]^2$, by equation (11.4). Given either one, the other can be found from the

formula. $E_p(\mu)$ is given by equation (11.5) and E_{pmax} is given by equation (11.6). $E_p(\mu)$, for z not zero, is always less than $E(\mu)$ point for point. E_{pmax} is always less than E_{max}.

There is always some depth below which the variation of the pressure caused by the passage of a short period wave overhead is undetectable due to the design of the pressure recorder. For example a five foot high wave with a five second period produces a pressure variation of only one one hundredth of a foot at a depth of 125 feet. This variation is essentially undetectable. Any variation in the power spectrum at the surface under the conditions described above is undetectable for all μ greater than $2\pi/5$.

These arguments also follow in a slightly modified way for pressure recorders located in shallow water (see Chapter 12). Ewing and Press [1949] have commented on the problem of the interpretation of pressure records, and their explanation is correct in that the correction must be applied to the whole power spectrum as indicated in equation (11.4).

Everything that has been said about records of the sea surface is true also about pressure records. The probability distribution of points of a pressure record is Gaussian. An equation similar to equation (7.33) can be written for the pressure distribution simply by substituting $P(t_1)$ for $\eta(t_1)$ and E_{pmax} for E_{max}. In addition, the pressure record contains less of the non-linear effects which cause an asymmetry of the distribution for the free surface.

The potential function and the velocity field

Given the pressure field and equation (2.7) and (2.9), then by the methods of equation (11.1) and (11.2), the potential function

Additional Properties of a Short Crested Gaussian Sea Surface in Infinitely Deep Water

$$\phi = -\int_0^{\infty}\int_{-\frac{\pi}{2}}^{\frac{\pi}{2}} \sin\left[\frac{\mu^2}{g}(x\cos\theta + y\sin\theta) - \mu t + \psi(\mu,\theta)\right] \sqrt{\frac{g^2 e^{2\mu^2 z/g}}{\mu^2}\left[A_2(\mu,\theta)\right]^2}\, d\theta\, d\mu \tag{11.7}$$

$$u = -\frac{\partial\phi}{\partial x} = \int_0^{\infty}\int_{-\frac{\pi}{2}}^{\frac{\pi}{2}} \cos\left[\frac{\mu^2}{g}(x\cos\theta + y\sin\theta) - \mu t + \psi(\mu,\theta)\right] \cdot \cos\theta \sqrt{\mu^2 e^{2\mu^2 z/g}\left[A_2(\mu,\theta)\right]^2}\, d\theta\, d\mu \tag{11.8}$$

$$v = -\frac{\partial\phi}{\partial y} = \int_0^{\infty}\int_{-\frac{\pi}{2}}^{\frac{\pi}{2}} \cos\left[\frac{\mu^2}{g}(x\cos\theta + y\sin\theta) - \mu t + \psi(\mu,\theta)\right] \cdot \sin\theta \sqrt{\mu^2 e^{2\mu^2 z/g}\left[A_2(\mu,\theta)\right]^2}\, d\theta\, d\mu \tag{11.9}$$

$$w = -\frac{\partial\phi}{\partial z} = \int_0^{\infty}\int_{-\frac{\pi}{2}}^{\frac{\pi}{2}} \sin\left[\frac{\mu^2}{g}(x\cos\theta + y\sin\theta) - \mu t + \psi(\mu,\theta)\right] \sqrt{\mu^2 e^{2\mu^2 z/g}\left[A_2(\mu,\theta)\right]^2}\, d\theta\, d\mu \tag{11.10}$$

$$\overline{K.E.}^{yt} = \overline{P.E.}^{yt} = \lim_{\substack{\bar{y}\to\infty \\ \bar{T}\to\infty}} \int_{t^*}^{t^*+\bar{T}} \int_{y^*}^{y^*+\bar{y}} \int_{-\infty}^{0} \frac{\rho}{2}(u^2+v^2+w^2)\, dz\, dy\, dt = \frac{\rho g}{4} E_{max} \tag{11.11}$$

$$u(t,z) = \int_0^{\infty} \cos(\mu t + \psi(\mu)) \sqrt{\mu^2 e^{2\mu^2 z/g}\left[D(\mu)\right]^2}\, d\mu = \int_0^{\infty} \cos(\mu t + \psi(\mu)) \sqrt{dF(\mu)} \tag{11.12}$$

where $$\left[D(\mu)\right]^2 = \int_{-\frac{\pi}{2}}^{\frac{\pi}{2}} \left[A_2(\mu,\theta)\right]^2 (\cos\theta)^2\, d\theta \tag{11.13}$$

and $$F(\mu) = \int_0^{\mu}\int_{-\frac{\pi}{2}}^{\frac{\pi}{2}} (\mu^*)^2 e^{2(\mu^*)^2 z/g}\left[A_2(\mu^*,\theta)\right]^2 (\cos\theta)^2\, d\theta\, d\mu^* \tag{11.14}$$

for the motion can be deduced immediately by integration of the variable part of the pressure with respect to time. The potential function is then given by equation (11.7). The u, v, and w velocity components can then be found immediately from the potential function and they are given by equations (11.8), (11.9), and (11.10). Note that $u_x + v_y + w_z = \varphi_{xx} + \varphi_{yy} + \varphi_{zz} = 0$, and the equation of continuity and, consequently, the potential equation are automatically satisfied for any functional form for $[A_2(\mu,\theta)]^2$.

The kinetic energy integrated over depth and averaged over y and t at any x is then given by equation (11.11). This is, of course, to be expected from Lamb [1932]. The proof will be left to the reader. The techniques of Chapter 9 can be employed. It can also be proved that the kinetic energy integrated over depth and averaged over t at any fixed point is also given by $\rho g E_{max}/4$. The proof follows by the application of the methods of Chapter 10.

The u component of the velocity for a fixed x and y and for any depth, z, can be written as a stationary Gaussian Integral as a function of time as given by equation (11.12). The functions, $[D(\mu)]^2$ and $F(\mu)$, are given by equations (11.13) and (11.14). The u velocities decrease in range with depth and change back and forth more slowly with time at greater depths. A graph of u as a function of time for some fixed depth, z, would look like a pressure record as the velocity shifts back and forth. However the power spectrum of the u velocity record would not have the same shape as the power spectrum of the pressure record for the same short crested wave system passing overhead. The interrelations are given by equations (11.14) and (11.4).

The cumulative power density of the u component of the velocity must be bounded as stated by equation (11.15). Equation (11.14) shows that for z not equal to zero, the term, $\exp[2(\mu^*)^2 z/g]$, can cause $F(\mu)$ to be bounded for all μ even if $[A_2(\mu,\theta)]^2$ is of a form in which E_{max} is unbounded. Thus any admissible $[A_2(\mu,\theta)]^2$ which has a bounded E_{max} must also result in reasonable velocities below the surface.

For z equal to zero in the equations for u, the equations give values for the surface water velocities due to the waves. It is true that the crest particle velocities occur at values of z greater than zero and the trough particle velocities occur at values of z less than zero, but such refinements are not justified in a linearized theory.

In equation (11.14), consider the integration for the case where z is zero. Suppose that the integration over μ and θ for μ less than μ_K is bounded. Also suppose that $[A_2(\mu,\theta)]^2$ can be expressed in a series form for μ greater than μ_K such that

$$[A_2(\mu,\theta)]^2 = f_1(\theta)/\mu + f_2(\theta)/\mu^2 + f_3(\theta)/\mu^3 + f_4(\theta)/\mu^4 + \ldots.$$

Then the integration over θ of this series times $(\cos\theta)^2$ must yield constant or zero values such that

$$[D(\mu)]^2 = C_1/\mu + C_2/\mu^2 + C_3/\mu^3 + C_4/\mu^4 + \ldots.$$

It then follows that $\mu^2[D(\mu)]^2 = C_1\mu + C_2 + C_3/\mu + C_4/\mu^2 + \ldots.$

Now, integration of $\mu^2[D(\mu)]^2$ from μ_K to infinity in the above form would yield infinitely large values of F_{max} unless C_1, C_2, and C_3 were zero. Therefore, they must be zero or else the power integral will break down and predict infinitely strong u velocity components

Additional Properties of a Short Crested Gaussian Sea Surface in Infinitely Deep Water

$$\lim_{\mu\to\infty} F(\mu) = F_{max} < M \qquad (11.15)$$

$$\lim_{\mu\to\infty} \mu^3 \left[A_2(\mu,\theta)\right]^2 = 0 \qquad (11.16)$$

$$\eta_x(x,y,t) = -\int_0^{\infty}\int_{-\frac{\pi}{2}}^{\frac{\pi}{2}} \sin\left(\frac{\mu^2}{g}(x\cos\theta + y\sin\theta) - \mu t + \psi(\mu,\theta)\right)\cos\theta \sqrt{\frac{\mu^4}{g^2}\left[A_2(\mu,\theta)\right]^2}\, d\theta\, d\mu \qquad (11.17)$$

$$\eta_{xx}(x,y,t) = -\int_0^{\infty}\int_{-\frac{\pi}{2}}^{\frac{\pi}{2}} \cos\left(\frac{\mu^2}{g}(x\cos\theta + y\sin\theta) - \mu t + \psi(\mu,\theta)\right)(\cos\theta)^2 \sqrt{\frac{\mu^8}{g^4}\left[A_2(\mu,\theta)\right]^2}\, d\theta\, d\mu \qquad (11.18)$$

$$\lim_{\mu\to\infty} \mu^9 \left[A_2(\mu,\theta)\right]^2 = 0 \qquad (11.19)$$

$$\overline{W.P.}^{yt} = \lim_{\substack{\bar{t}\to\infty \\ \bar{y}\to\infty}} \int_{y^*}^{y^*+\bar{y}} \int_{t^*}^{t^*+\bar{t}} \int_{-\infty}^{0} P(x,y,z,t)\, U(x,y,z,t)\, dz\, dt\, dy$$

$$= \frac{\rho g}{2} \int_0^{\infty}\int_{-\frac{\pi}{2}}^{\frac{\pi}{2}} \cos\theta \left[A_2(\mu,\theta)\right]^2 \mu \int_{-\infty}^{0} e^{2\mu^2 z/g}\, dz\, d\theta\, d\mu$$

$$= \frac{\rho g^2}{4} \int_0^{\infty}\int_{-\frac{\pi}{2}}^{\frac{\pi}{2}} \frac{\cos\theta \left[A_2(\mu,\theta)\right]^2}{\mu}\, d\theta\, d\mu \qquad (11.20)$$

$$\lim_{\mu\to 0} \frac{\left[A_2(\mu,\theta)\right]^2}{\mu} < M \qquad (11.21)$$

Plate IIX

all of the time. The constants, C_1, C_2, and C_3 were determined from $f_1(\theta)$, $f_2(\theta)$, and $f_3(\theta)$. These functions of θ must be positive everywhere or else $[A_2(\mu,\theta)]^2$ can have negative values. Therefore $f_1(\theta)$, $f_2(\theta)$, and $f_3(\theta)$ must be zero. Therefore for values of μ greater than μ_K, the power spectrum must be of the form $f_4(\theta)/\mu^4$ (at least) such that when multiplied by μ^3, it goes to zero as μ approaches infinity. A better way to state this requirement is given by equation (11.16) because fractional powers in the series expansion are then also possible.

The results that have just been obtained can be interpreted in a very easy way by considering sea surfaces composed of purely periodic ten second waves, purely periodic five second waves, purely periodic two and one half second waves, and so on. If the various separate wave trains are all of the same height then the particle velocities at the surface are twice as great in the five second waves as in the ten second waves and four times as great in the two and one half second waves as in the ten second waves. If a condition such as the one just derived is not imposed, very strong velocities must result.

The slope and curvature of the sea surface

These power integrals can also be differentiated and integrated with respect to the time and space variables. The slope of the sea surface in the x direction as a function of time and space variables is given by equation (11.17). By the methods of Chapter 10, this equation can be reduced to a function of time at any point. It then follows that the slope in the x direction is given by an integral of the form of equation (7.1) except that the power spectrum is

given by $\mu^4[D(\mu)]^2/g^2$ instead of $[A(\mu)]^2$. The slopes are therefore distributed according to a normal distribution with a mean of zero and a variance related to the integral of the function just given above from zero to infinity.

The curvature of the sea surface in the x direction is given by equation (11.18). The curvature as a function of time at a fixed point is, from the same reasoning as used above, distributed according to a normal distribution with a zero mean and a standard deviation related to the integral from zero to infinity of $\mu^8[D(\mu)]^2/g^2$.

Infinite values for the curvature of the sea surface mean that at that point on the sea surface a sharp breaking angle occurs in the wave profile. Equation (11.18) shows that these sharp curvature changes are associated with the short waves (or the higher wave frequencies). If the integral is to behave properly, the condition given by equation (11.19) must be imposed.

Wave power and energy transfer

Consider the yz plane which results from picking a fixed value of x. The work being done on this plane when averaged over y and t and integrated over depth is the wave power or the flux of energy in ergs/sec per centimeter of length along the y axis. The equation given in Lamb for section 237(equation 10) can be modified to yield the first expression in equation (11.20). Substitution of equations (11.2) and (11.8), followed by the indicated integrations and limiting processes, then yields the average rate of transmission of wave energy across the yz plane per unit length of the y axis. Without the cosθ term, equation (11.20) would represent the total

outflow of wave energy from the storm area. From arguments similar to those which have been used above, the wave power will not be bounded unless equation (11.21) holds.

Equation (11.20) has a particularly important application in wave forecasting theory. At the forward edge of a storm at sea, it measures the energy which is being transmitted into the area of calm by the waves as they leave the edge of the storm area. The storm winds in the atmosphere by some mechanism transfer energy to the waves in the generating area. The energy in the wave motion in the generating area flows out of the generating area at a rate given by equation (11.20) (plus a component in the y direction). The important point is that in order to maintain the same amplitude of the power spectrum near μ equal to $2\pi/10$ that is maintained near μ equal to $2\pi/5$, the atmosphere must transmit twice as much energy per unit time to the generating area near frequencies given by μ equal to $2\pi/10$ than is required near μ equal to $2\pi/5$.

Consider, for example, two power spectra. One is given by $[A_2(\mu,\theta)]^2$ equals a constant over the area bounded by μ equal to $2\pi/11$ and $2\pi/9$ and by θ equal to $\pm\,\pi/36$. The other is given by $[A_2(\mu,\theta)]^2$ equals the same constant over the area bounded by μ equal to $2\pi/5.24$ and $2\pi/4.74$, and by θ equal to $\pm\,\pi/36$. The two power spectra have the same band width and the same value of E_{max}, but were such power spectra actually to exist over a generating area, twice as much energy would have to be transmitted to the sea surface by the atmosphere in order to maintain the waves for the first power spectrum than would have to be transmitted to the surface in order to maintain the second power spectrum. Energy

transmission for low values of μ is much greater than for high values of μ and it is therefore more difficult for the storm winds to maintain that part of a power spectrum which applies to low values of μ .

A limitation on the power spectrum guessed from non-linear considerations

It is dangerous to attempt to apply non-linear criteria to linearized systems. The linearized theory presented so far has gone a long way toward explaining the properties of actual storm generated ocean waves, and it appears to give consistent results. A linearized theory usually has one fault in that the theory in itself seldom yields information on when it will fail.

For example, the requirement that E_{max} be bounded was imposed in Chapter 7 for the first time and equations such as equation (11.15), (11.16), (11.19), and (11.21) have been deduced from this property and other considerations. However $[A_2(\mu,\theta)]^2$ is still undetermined to within a constant factor. That is, if a given functional form for $[A_2(\mu,\theta)]^2$ satisfies all of the requirements which have been deduced, it is still undetermined to within a constant factor because it can be multiplied by a factor of 10 or 100 or 1000 and it would still satisfy all of these requirements.

This is, of course, against good sense and against the initial assumption that the disturbance was small. There is no way to tell when the theory will get seriously out of hand for large magnitudes for the function from any of the previously given formulas.

It is possible to make an educated guess about when the theory will certainly fail, and sometimes an educated guess is a very good

thing to have in lieu of actual knowledge. It is known from non-linear wave theory (Lamb [1932], sec. 250, see footnote on the work of Michell, and also Davies [1951]) that, for a purely periodic wave of finite height, the ratio of the wave height to the wave length cannot exceed one seventh. Michell obtained a value of 1/7.05, and Davies' [1951] most recent results are given by a value of 1/6.914. Equation (11.22)uses the value 1/7 because the result is to be only an approximation. Suppose that all of the power in the power spectrum for μ greater than μ_K were concentrated in one purely periodic wave with a wave length determined by μ_K. Then certainly the integral given on the left in equation (11.23) is less than the integral given in the middle and there is reason to believe that they both must be less than the value, 1/49. The longest possible wave length has been taken on the left in this equation, and the waves would certainly be very steep if $[A_2(\mu,\theta)]^2$ had major contributions for values of μ very much larger than μ_K. Of course nothing can be said about how these short waves combine with the longer waves for μ less than μ_K in the non-linear case, but if $[A_2(\mu,\theta)]^2$ were identically zero for μ less than μ_K, equation (11.23) would still have to hold. It would seem that any added disturbance for μ less than μ_K would only serve to increase the instability of the waves for μ greater than μ_K.

If these arguments are valid, then equation (11.24) follows from equation (11.23). It states that the power in $[A(\mu)]^2$ from μ_K to infinity must be less than some constant times μ_K^{-4}. In terms of T_K, this power must be less than $328T_K^4$.

For small values of μ_K, this result gives a larger possible

Additional Properties of a Short Crested Gaussian Sea Surface in Infinitely Deep Water

From non linear considerations, for a purely periodic wave $\frac{H^2}{L^2} > \frac{1}{49}$ (II.22)

which suggests $$\int_{-\frac{\pi}{2}}^{\frac{\pi}{2}}\int_{\mu_K}^{\infty} \frac{\mu_K^4\left[A_2(\mu,\theta)\right]}{[2\pi g]^2} d\mu d\theta < \int_{-\frac{\pi}{2}}^{\frac{\pi}{2}}\int_{\mu_K}^{\infty} \frac{\mu^4 A_2(\mu,\theta)}{4\pi^2 g^2} d\mu d\theta < \frac{1}{49} \quad \text{(II.23)}$$

$$\text{or} \int_{\mu_K}^{\infty}\left[A(\mu)\right]^2 d\mu = \int_{-\frac{\pi}{2}}^{\frac{\pi}{2}}\int_{\mu_K}^{\infty}\left[A_2(\mu,\theta)\right]^2 < \frac{4\pi^2 g^2}{49\mu_K^4} = \frac{g^2}{296\pi^2} T_K^4 = 328\, T_K^4 \text{ cm.}^2 \quad \text{(II.24)}$$

$$\int_{\mu_K}^{\infty} \frac{c_4}{\mu^4} d\mu = -\frac{c_4}{3\mu^3}\Big|_{\mu_K}^{\infty} = \frac{c_4}{3\mu_K^3} < \frac{4\pi^2 g^2}{49\mu_K^4} \quad \text{(II.25)}$$

$$c_4 < \frac{6\pi g^2}{49} T_K = \frac{12\pi^2 g^2}{49\mu_K} \quad \text{(II.26)}$$

$$\lim_{\mu\to\infty} \mu^M\left[A_2(\mu,\theta)\right]^2 = 0 \quad \text{(II.27)}$$

Some Sample Cross Correlation Functions

$$\chi(p) = \lim_{\bar{T}\to\infty} \frac{1}{\bar{T}} \int_{t^*}^{t^*+\bar{T}} \eta(t)\ P(z,t+p)dt \quad \text{(II.28)}$$

$$\chi(\rho) = \lim_{\bar{x}\to\infty} \frac{1}{\bar{x}} \int_{x^*}^{\bar{x}^*+\bar{x}} \eta(y,x)\,\eta(y\ ,x+\rho)dx \quad \text{(II.29)}$$

Plate IX

value for the power present. For T_K equal to 10 seconds, the power could be of the order of $3.28\ 10^6$ cm^2 (equivalent to a purely sinusoidal wave approximately eighteen meters high) between $2\pi/10$ and infinity. For T_K equal to 1 second, the power between 2π and infinity could be of the order of 328 cm^2 (equivalent to a purely sinusoidal wave 18 cm high).

Of course, for much smaller values of T_K, these formulas begin to lose significance because the elemental waves are no longer gravity waves but capillary waves. The modification of these equations by the appropriate forms for capillary waves might yield additional theoretical information about the high end of the spectrum.

The bound given on $[A(\mu)]^2$ by these considerations is most likely an overestimate as to when the linear theory fails. That is, if the inequality is not satisfied, then the linear theory certainly fails, but if the inequality is satisfied, then the linear theory may still fail in one or more theoretical aspects. In addition, it would be fairly safe to predict that functional forms for $[A(\mu)]^2$ will never be found in nature which fail to satisfy the requirements given in equation (11.24) because were the winds to attempt to build such a wave system, the system would be destroyed as fast as it is formed by breaking and turbulence at the crests. The "outsize" waves predicted by The Gaussian distribution would presumably be very unstable.

The shape and properties of the possible power spectra

Equations (11.16), (11.19), (11.21) and (11.24) taken together yield a considerable amount of information on what power spectra are possible, on the shape of the power spectra, and on the appear-

ance of the sea surface. The shapes of the power spectra will be discussed first at the high frequency end and then at the low frequency end in terms of what power spectra are possible. This will also permit a discussion of the appearance of the sea surface as a by-product.

Equation (11.16) and (11.24) combined with the discussion given in the paragraphs on the potential function and the velocity field show from equation (11.25) (if $[A_2(\mu,\theta)]^2$ has a series expansion) that the constant, C_4, must be less than the value given in (11.26). For μ_K equal to 2π, C_4 must be less than $117{,}600\pi$, and the largest possible value for the term (when μ equals 2π) is equal to $117{,}600\pi/(2\pi)^4$ or 236 cm^2 sec. With the above value for C_4, the power between 2π and 3π as computed from (11.25) with different limits of integration is very nearly 328 cm^2, and there is little power above the value 3π.

At the high end of the frequency spectrum, then, the spectrum must die down in amplitude at least as fast as C_4/μ^4. For moderate values of μ, the spectrum can get to be quite high but it must always satisfy equation (11.24).

Equation (11.21) applies to the low end of the frequency spectrum. Especially in the source region, it states that the flow of energy across the forward edge of the storm must be bounded. Some results from the formulas given in Chapter 9 also apply here. For a wave system over a fetch 250 km long, seventeen hours after the winds cease, the power spectrum at the edge of the fetch will no longer contain values of μ less than $2\pi/5$. Waves therefore die down in the storm area very rapidly as soon as the winds cease

(see figure 25). Conversely, tremendous amounts of energy have to be supplied to the sea surface from the winds in the storm overhead. For a steady state, the energy supplied per second from the atmosphere to the waves must balance the energy dissipated per second by the waves in breaking at the crests and the energy per second which flows out of the forward edge of the storm area as the waves propagate into the area of calm. The balance must hold for each possible elemental area in a net of the μ ,θ plane.

At the low end of the power spectrum, very large amounts of energy are leaving the generating area every second. Consequently the lower the value of μ , the more difficult it is for the storm to maintain a wave of any appreciable amplitude. Therefore, as μ is decreased the power spectrum must pass through some peak value and then begin to decrease as μ gets close to zero.

If the oceans were infinitely deep these considerations would hold exactly and equation (11.21) would have to hold exactly. The oceans are only about 3000 meters deep. A wave 6000 meters long is still essentially in deep water. This corresponds to a period of 61.7 seconds or a μ of $2\pi/61.7$ seconds. Thus for μ less than $2\pi/61.7$ seconds, these arguments do not hold exactly. However, the rate of energy flow out of a generating area is still tremendous for μ less than $2\pi/62$ and the arguments are still qualitatively valid since the ocean is not really shallow water ($C \cong \sqrt{gh}$) until the period of the waves becomes about 1330 seconds. The point, $\mu = 2\pi/1330$, is very close to the origin in all of the forecasting curves which have been shown.

Sea surface "glitter"

So far no claim that equation (11.19) must hold has been put forward. The sea surface could be covered by many small facets and at many points the curvatures can be sharp. However, intuitively at least, equation (11.18) should have a meaning everywhere and this is not the case unless equation (11.19) holds. If equation (11.19) holds, then C_4 must be zero. In addition, in the same series discussed above, C_5, C_6, C_7, C_8, and C_9 must all be zero and for some μ greater than μ_K the series must be of the form $\mu^8[A_2(\mu,\theta)]^2(\cos\theta)^2 = f_{10}(\theta)/\mu^2$ plus higher order terms.

The results show that there is a tendency for the high frequency components to produce many sharp facets on the sea surface. These facets can be observed in fresh waves from a generating area and they are particularly noticeable in the photograph which has been chosen for the frontispiece. Any light breeze can superimpose a high frequency spectrum on a swell and it is believed that these considerations account very nicely for the sea surface "glitter."

Final form for the power spectrum

If it is required that all derivatives of the sea surface, the velocity field, and the pressure field have a defined power spectrum and a defined power integral, then the requirement posed by equation (11.27) must be fulfilled for any integer value of M, no matter how large. No polynomial in $(1/\mu)^n$ can satisfy this requirement. Therefore $[A_2(\mu,\theta)]^2$ cannot be represented by a fraction consisting of polynomials in μ in the numerator and denominator. The power spectrum must therefore be either some

entire transcendental function capable of satisfying equation (11.27) and equation (11.24) for μ greater than μ_K if it is to have a value for all μ or it must be identically zero for μ greater than some value. The functions given in the examples in Chapter 9 satisfy equation (11.27) [and therefore (11.19) and (11.16)]. When they were manufactured, condition (11.24) was not known. It might be an interesting problem for the reader to see if they satisfy equation (11.24) for all values of μ_K.

The use of autocorrelation functions

The non-normalized autocorrelation function given in equation (10.26) was used to find the power spectrum. In its own right it is an extremely important function in wave theory because it permits short range predictions of what the next few waves will be like. The non-normalized autocorrelation function of a wave record dies down to zero for large values of p and it is very small, for example, for p equal to about 180 seconds for a power spectrum from a "sea" record. This means that what occurs at the point of observation three minutes after, say, a crest passes that point has very little to do with the fact that a crest passed three minutes ago. Stated another way, it is impossible to predict whether a crest or a trough will be passing the point of observation three minutes after a given time of observation. Note that the power spectrum of the wave system tells us a great deal about the whole wave record, about the characteristics of the record, and about the "sea" and "swell" properties. However nothing can tell us the exact shape of the wave record three, ten, twenty or thirty minutes into the future.

In contrast, if a wave record could be represented by any number of discrete spectral components with, say, four place accuracy for the spectral periods, then it is theoretically possible to predict the wave records into the future for a long time. For example, suppose that a wave record were actually composed of three sine waves of amplitudes A_1, A_2, and A_3, with periods of 8.75, 10.35, and 14.10 seconds, respectively, and that the numbers actually mean that the periods are between 8.745 and 8.755, 10.345 and 10.355, and 14.095 and 14.105. Then after one thousand seconds (17 minutes), the greatest possible predicted phase error would be 24 degrees. At a point in the future one thousand seconds ahead at which, say, theoretical positive cosinusoidal reinforcement is to occur the predicted amplitude would have to be between $A_1 + A_2 + A_3$ and $A_1\cos 23.5° + A_2\cos 16.8° + A_3\cos 9°$. The autocorrelation function implies that such accuracy is fallacious, that a wave record cannot be predicted that far into the future for "sea" conditions, and that the sea surface cannot possibly be composed of discrete spectral components.

Wiener [1949] has given the mathematical procedure for predicting the future behavior of a stationary time series given its past. From the past, the first step is to find an estimate of the autocorrelation function. The autocorrelation function can then be used to determine the kernal of an integral equation such that when the past of the record is multiplied by the kernal and integrated over past time, a number results which is the best possible forecast for the value which will occur, say, thirty seconds into the future. The best possible forecast is in the least square sense; that is,

the difference between the forecasted value and the actual value squared is a minimum over all forecasts. If the autocorrelation function is essentially zero from lags of three minutes onward, then the forecast would be a zero amplitude disturbance at all times beyond three minutes in the future. This forecast would be correct in the least squares sense because the second moment about the mean (zero) is the smallest second moment possible and in the sense that the autocorrelation function implies that what will happen in three minutes has nothing to do with what is happening.

If it ever becomes essential to know thirty seconds in advance that a big wave is coming then it is possible to imagine an electronic circuit constructed along the lines of the one described by Lee [1949] which will graph the wave record as it will occur 30 seconds in the future given the present wave record. Note also figure 22 in Lee's paper. The random voltages shown look exactly like wave records!! The machine described by Lee [1949], if one imagines it applied to wave forecasts would only predict the records about three seconds in advance.

A ship at sea is acted upon by a Gaussian wave system. Therefore it pitches, rolls, and rises and falls according to a Gaussian law. The continuous record of, say, the inclinometer is therefore a temporarily homogeneous Gaussian record, and from the autocorrelation function of the inclinometer record it is therefore possible to predict from the past when the next big roll of the ship will occur.

A very fruitful line of future research will be to apply the methods given by John [1949] to a Gaussian sea surface and determine the movement of floating objects on the sea surface in response to

the waves. John [1949] has solved the problem for a purely periodic wave. His solution is given in the form of a Fredholm integral equation (which may or may not be solvable itself). Stoker, in a recent conference, suggested more direct methods which could yield immediate practical results. By the principals of Chapters 9 and 10 these results can be extended to the Gaussian case.

Cross correlation functions

Another important tool for the study of ocean waves is the cross correlation function. There are many possible cross correlation functions which can be constructed. For example, $\chi(p)$, given by equation (11.28), gives the cross correlation between the height of the free surface at a fixed point and the pressure recorded by a pressure recorder at some depth, z, below the surface at that same point. As another example, equation (11.29) gives the relationship between the free surface at two different values of y at a fixed time.

With these cross correlation functions, many properties of the sea surface, the velocity component fields, and the pressure fields can be interrelated and studied. A detailed study of equation (11.28) would probably show that the deeper the pressure recorder the less it reflects the passage of high short "apparent" period waves overhead and that it is easily possible for a pressure recorder to record a crest when actually a trough is passing overhead (or conversely). The cross correlation functions must be studied by carefully keeping the same net and the same $\psi(\mu,\theta)$ for each term in the net for the two functions being studied. Although values are Gaussian, for example, an accidental high crest is related to an accidental high

u velocity component at that same point and time of observation.

Lines for future research

All of the things suggested above on the autocorrelation functions and the cross correlation functions cannot be treated here in detail because they require very extensive mathematical abilities and they are sidelights on the main problem of wave analysis, wave propagation, and wave refraction. Their importance is obvious, and they suggest many avenues for future research and investigation.

Chapter 12. WAVE REFRACTION IN THE TRANSITION ZONE

Introduction

The assumption that the oceans are infinitely deep have proved very useful so far in the study of ocean waves. For all practical purposes, the errors involved are not important. Sooner or later, somewhere, the disturbance is dissipated by the breaking of the waves on a coastline. Waves leave the deep parts of the oceans and travel finally to the shallow waters bordering a coast of an island or a continent. In the shallower waters, if the depth is constant over a relatively large area, the wave crest speed of a purely sinusoidal wave is given by equation (12.1). But wave refraction complicates the problem, and it is necessary to treat the wave crest speed as if it were a slowly varying function of position. There are varying degrees of accuracy with which the problem of wave motion over an area where the depth is less than, say, one half the wave length of the lowest important spectral component, can be treated. These methods will be discussed in this chapter.

As the waves advance into an area where the effect of depth is important, a large area can be found such that the results of the previous chapters can be extended to explain the observed patterns and aerial photographs. Later, as the waves near the breaker zone, a transformation often appears to occur which substantiates some of the results of Munk [1949] on Solitary Wave Theory. Finally, the waves peak up and break.

The breaking wave is a phenomenon of the non-linearity of the original equations of motion. All methods of wave analysis and wave

refraction which are based upon the linear theory fail in one or more important aspects in the breaker zone. Therefore the methods developed in this paper cannot be applied to the breaker zone.

Between deep water and the coast there will first be found a zone which will be referred to in this paper as the transition zone. Between the transition zone and the coast there is a possibility of a solitary wave zone, a shallow water wave zone, and a breaker zone. If boundaries between the transition zone and the above three zones can be defined, then in this paper the theory will apply to the transition zone as marked by deep water on one side and the boundary of that zone (of the above three zones) which is farthest from the coast. Non-linear effects of great importance must be present in these near-shore zones, and they will not be treated in this paper.

It might also be noted that conditions can occur in which the solitary wave zone, the shallow water zone, and the breaker zone would not occur. Also any two of the above zones or any one of the above zones might be missing. For example, waves approaching a vertical cliff rising sheerly out of a depth of forty feet at the edge of a bottom of variable depth could be reflected back out to deep water without ever undergoing any of the above suggested modifications.

The invariance of discrete spectral periods

Consider the following experiment in a very long deep wave tank. Waves with a period of exactly two seconds are generated in a forty foot depth at one end of the tank. The water for all practical purposes is infinitely deep, and the waves can be expressed as a

function of x and t alone at that end of the tank. Twenty miles away let the depth shoal gradually and linearly over a distance of ten miles to a final depth of five feet. For another twenty miles let the depth remain at five feet and then let the tank be ended by a perfect wave absorber without any reflection. Suppose also that the generator has been running for about two months so that all transient effects can be ignored. Finally let the amplitude of the waves at the generator be two inches so that the small height assumption can be used as an approximation.

Now, at a distance of five miles from the generator, the waves will have a speed given by $C^2 = g^2T^2/4\pi^2 = gL/2\pi$. Exactly one sinusoidal crest will pass the point of observation every two seconds. The wave record will be essentially a pure sine wave if observed at a fixed point. The period of the wave will be exactly two seconds.

At a distance of forty five miles from the generator, the waves will have passed over the sloping bottom, and at a distance of fifteen miles from the slope, since the deep water wave length is only one two hundredth and sixty fourth of a mile, the waves in the region ought to be again nearly sinusoidal in form and the crests ought to be traveling again with a constant speed. The crest speed ought to be given by equation (12.1) from classical theory.

A long time ago in Chapter 2, under the assumption that the motion was purely periodic with one discrete spectral period, a periodicity factor in time for depth still variable was split off from the potential equation. The above experiment has been designed to show why this assumption is valid. Suppose that at this second point of observation the period of the wave is recorded. The period

must be exactly two seconds.

Suppose that the period is not exactly two seconds at the second point of observation. Suppose, for example, that the period is really 2.01 seconds. Near the generator the period is two seconds. Each periodic motion at the first point of observation means that one wave crest has progressed toward the second point of observation. In the next one hundred hours, then, 180,000 waves will pass the first point of observation. At the second point of observation, where the period is assumed (erroneously) to be 2.01 seconds only 179,104 waves will pass during the time of observation. Thus 896 waves left the first point which did not arrive at the second point. But at the start, it was assumed that the motion had settled down to a steady state; and now it is found that the number of wave crests between the two points is continuously increasing. The assumption that the period is not the same is therefore wrong. Therefore the period at the second point of observation must be exactly the same as at the first point of observation.

It might be remarked that a formal exact mathematical solution to the experiment just described has never been obtained. The works of Stoker [1947] and Eckart [1951] come close to solving the problem, but Stoker's solution for a linear sloping beach although exact, as far as the linear theory goes, is not quite a solution to this problem and Eckart's methods would yield only an approximation to the true solution.

Finally, though, the important point is that whatever solution is found the period of the motion at the second point must be the same as at the first point. Also the wave speed at the second point

will be essentially given by equation (12.1).

Waves in water of constant depth:

Consider a point in the transition zone where the depth is constant over a rather large area. The problem is to represent the sea surface and the other desired quantities in the vicinity of that point. None of the previous representations are correct in the transition zone except that the wave record as a function of time is still given by the same general function of time discussed in Chapter 7. In particular the methods given in Chapter 10 for the determination of power spectra as a function of μ and θ, will not apply to waves measured in the transition zone.

Equation (12.1) gives the speed of the wave crests as a function of the wave length for a pure sine wave in water of depth, H. Equation (12.2) relates the speed of the wave crests to the wave length and the wave period. The period is independent of depth. From equation (12.1) and (12.2), an equation for the wave length of a wave in water of depth H can be found in terms of the wave period. A conversion of spectral periods to spectral frequencies then will permit integrals over power spectra similar to those considered before.

If the expression for C in terms of L and μ in equation (12.2) is substituted into equation (12.1), equation (12.3) is the result. Rearrangement then yields equation (12.4) in which the wave length in water of depth, H, is given as a function of the spectral frequency and the depth.

Usually (12.4) has been solved graphically (with a slightly different notation). Sverdrup and Munk [1944] give graphs of L/L_o (i.e. $Lg/2\pi\mu^2$) as a function of $2\pi H/L_o$. The Beach Erosion Board

Waves in Water of Constant Depth

$$c^2 = \frac{gL}{2\pi} \tanh \frac{2\pi H}{L} \qquad (12.1)$$

$$c = \frac{L}{T} = \frac{L\mu}{2\pi} \qquad (12.2)$$

$$\frac{L\mu^2}{2\pi} = g \tanh \frac{2\pi H}{L} \qquad (12.3)$$

$$\frac{2\pi}{L} = \frac{\mu^2}{g} \coth H \frac{2\pi}{L} \qquad (12.4)$$

$$\frac{2\pi}{L} = \frac{\mu^2}{g} \coth H \frac{2\pi}{L} \qquad (12.5)$$

$$\frac{2\pi}{L} = \frac{\mu^2}{g} \coth \left(H \frac{\mu^2}{g} \coth H \frac{2\pi}{L}\right) \qquad (12.6)$$

$$\frac{2\pi}{L} = \frac{\mu^2}{g} \coth \left(H \frac{\mu^2}{g} \coth \left(H \frac{\mu^2}{g} \coth H \frac{2\pi}{L}\right)\right) \qquad (12.7)$$

$$\frac{2\pi}{L} = \frac{\mu^2}{g} \coth \left(H \frac{\mu^2}{g} \coth \left(H \frac{\mu^2}{g} \coth \left(H \frac{\mu^2}{g} \coth H \frac{2\pi}{L}\right)\right)\right) \qquad (12.8)$$

$$\frac{2\pi}{L} = \frac{\mu^2}{g} \coth \left(H \frac{\mu^2}{g} \coth \left(H \frac{\mu^2}{g} \coth \left(H \frac{\mu^2}{g} \cdots\cdots\cdots\right)\right)\right) \qquad (12.9)$$

$$\frac{2\pi}{L} = \frac{\mu^2}{g} \operatorname{Itcoth}\left(H \frac{\mu^2}{g}\right) = \frac{\mu^2}{g} \mathrm{I}\left(H \frac{\mu^2}{g}\right) \qquad (12.10)$$

$$\operatorname{Itcoth}\left(H \frac{\mu^2}{g}\right) = \coth\left(H \frac{\mu^2}{g} \operatorname{Itcoth} H \frac{\mu^2}{g}\right) \qquad (12.11)$$

$$\mathrm{I} = \coth\left(H \frac{\mu^2}{g} \mathrm{I}\right) \qquad (12.12)$$

$$\frac{H\mu^2}{g} = \frac{1}{\mathrm{I}} \coth^{-1} \mathrm{I} \qquad (12.13)$$

Plate LXI

gives complete tables of the same ratio. However, given T, and H and a table of ordinary hyperbolic functions, it is possible to find the above length without recourse to these graphs and tables.

Equation (12.5) is equation (12.4) written down again. Substitute the expression for $2\pi/L$ on the right in (12.5) for the $2\pi/L$ under the hyperbolic cotangent on the right of equation (12.4). The result is equation (12.6). Again substitute the value of $2\pi/L$ in (12.5) into the far right of (12.6). The result is equation (12.7). Do it again. The result is equation (12.8). After an infinite number of substitutions the result is that $2\pi/L$ is given as a function of μ and H* alone on the right hand side of the equation. Thus, in a sense, equation (12.4) has been solved for $2\pi/L$ in terms of H and μ. The new function suggested by equation (12.9) is defined by equation (12.10) to be the Itcoth of $H\mu^2/g$, [or $I(H\mu^2/g)$]. The symbol, $\text{Itcoth}(H\mu^2/g)$, is to be read as the iterated hyperbolic cotangent of $H\mu^2/g$. It can also be pronounced easily just as it reads. The Itcoth appears to be a brand new function, never written down before.

The point of the new function is that substitution of $H\mu^2/g$ for $H2\pi/L$ at the far right in the iteration makes no error in the value of the function. In fact only seven or eight iterations yield three place accuracy for the Itcoth starting out with $H\mu^2/g$ instead of $H2\pi/L$ if $H\mu^2/g$ is fairly large. Near zero values, many more iterations are needed.

Table 17 illustrates this point. Let the depth be one eighth

---

*The usual notation for this symbol is h, but H is used here in order to avoid confusion with the h of Chapter 10.

Table 17. Computation of the Itcoth by Iteration

$$\text{Let } H = \frac{L_o}{8} \; ; \; \frac{\mu^2 H}{g} = \frac{2\pi H}{L_o} = \frac{2\pi L_o}{8L_o} = \frac{\pi}{4} = .785$$

Number of Iterations		
1		coth(.785) = 1.524
2	coth(.785)(1.524)	= coth(1.12) = 1.238
3	coth(.785)(1.238)	= coth(.972) = 1.333
4	coth(.785)(1.333)	= coth(1.05) = 1.282
5	coth(.785)(1.282)	= coth(1.006) = 1.309
6	coth(.785)(1.309)	= coth(1.028) = 1.294
7	coth(.785)(1.294)	= coth(1.0158) = 1.302
8	coth(.785)(1.302)	= coth(1.022) = 1.297

Therefore $1.297 < I(.785) < 1.302$;
if L_o were equal to 1000 feet and
if H were 125 feet, then L would be
1000/1.30 or L = 769.2 feet.

of the depth water wave length. Then $\mu^2 H/g$ equals $2\pi H/L_o$ which in turn yields $2\pi L_o/8L_o$ or the number $\pi/4$.

The value of $\pi/4$ to three figures is given by 0.785. The hyperbolic cotangent has the value 1.524 as shown in the first row. The second row gives the hyperbolic cotangent of 0.785 times 1.524. The true value of the Itcoth lies between the two numbers given by 1.524 and 1.238.

Eight iterations then yield the values given by row 7 and row 8. Within an error of one half of one percent the true value of the Itcoth for $\mu^2 H/g$ equal to $\pi/4$ is 1.30. Given that the wave length in deep water is 1000 feet, the depth would then be 125 feet

and the wave length at the depth of 125 feet would be 769.2 feet. Note that no special tables or graphs were used.

The Itcoth has an additional property which is given as equation (12.11). If the hyperbolic cotangent of the product of $H\mu^2/g$ and the Itcoth of $H\mu^2/g$ is formed, it will again equal the Itcoth of $H\mu^2/g$. This is shown by Table 17. If the Itcoth is treated as the dependent variable, I, equation (12.12) follows. The inverse of the equation then yields $H\mu^2/g$ as a function of I, and in equation (12.13), $H\mu^2/g$ is given as a function of I. The function given by equation (12.13) is graphed in figure 31. Other relationships of a useful nature are also given in the figure.

Since the wave length of a wave with a known spectral frequency (or period) has now been given as a function of that spectral frequency and the depth, H, of the water, it is now possible to write down the expression for the free surface for one pure sine wave, in water of constant depth, H. The free surface is given by equation (12.14) in which the constant spectral frequency is given by μ_I and the depth is H. It is easy to show that this expression reduces to the forms given before if H becomes infinite.

Equation (12.15) then yields the potential function. It is again easy to show that the potential function satisfies all required properties and that it reduces to the appropriate form in water of infinite depth.

The appropriate Gaussian systems then follow immediately from previous considerations. The free surface is given by equation (12.16). $E_{2H}(\mu,\theta)$ is the cumulative power distribution function for waves in water of depth, H. The function, $\psi(\mu,\theta)$ and the function, $E_{2H}(\mu,\theta)$

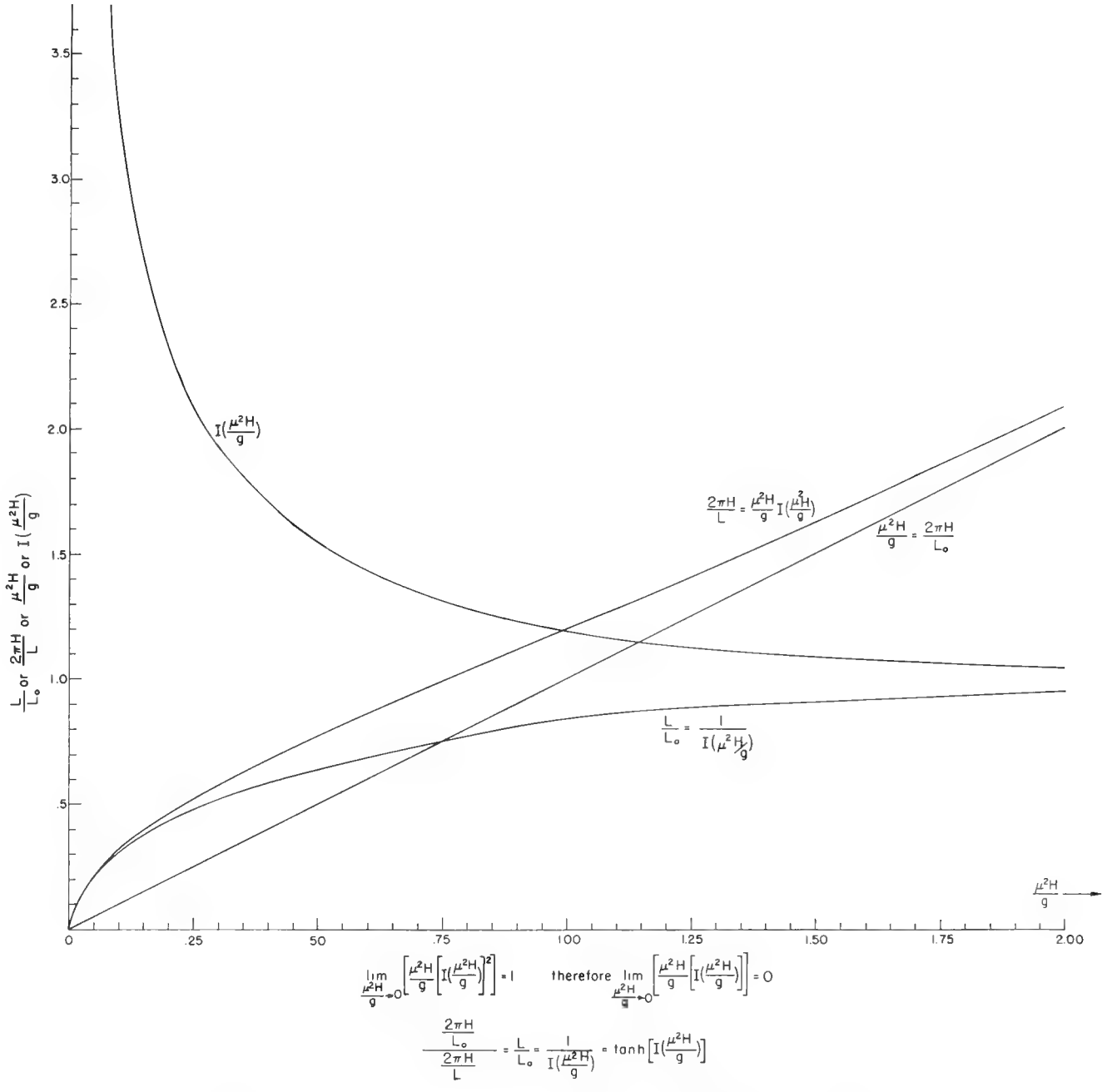

Figure 31. Graph of the Itcoth as a function of $H\mu^2/g$ and other related functions.

Waves in Water of Constant Depth

$$\eta(x,y,t) = A \cos\left[\frac{\mu_I^2}{g} I\left(H\frac{\mu_I^2}{g}\right)\left[x\cos\theta_1 + y\sin\theta_1\right] - \mu_I t + \delta\right] \tag{12.14}$$

$$\Phi(x,y,z,t) = -\frac{Ag}{\mu_I}\frac{\cosh\left[\frac{\mu_I^2}{g}\cdot I\left(H\frac{\mu_I^2}{g}\right)\cdot(H+z)\right]}{\cosh\left[\frac{\mu_I^2}{g}\cdot I\left(H\frac{\mu_I^2}{g}\right)H\right]}\cdot\sin\left[\frac{\mu_I^2}{g} I\left(H\frac{\mu_I^2}{g}\right)\left[x\cos\theta_1 + y\sin\theta_1\right] - \mu_I t + \delta\right] \tag{12.15}$$

Gaussian Systems

$$\eta(x,y,t) = \int_0^{\infty}\int_{-\frac{\pi}{2}}^{\frac{\pi}{2}} \cos\left[\frac{\mu^2}{g}\cdot I\left(H\frac{\mu^2}{g}\right)\left[x\cos\theta + y\sin\theta\right] - \mu t + \psi(\mu,\theta)\right]\cdot\sqrt{d^2 E_{2H}(\mu,\theta)} \tag{12.16}$$

$$\Phi(x,y,z,t) = \int_0^{\infty}\int_{-\frac{\pi}{2}}^{\frac{\pi}{2}} \frac{\cosh\left[\frac{\mu^2}{g}\cdot I\left(H\frac{\mu^2}{g}\right)\cdot(H+z)\right]}{\cosh\left[\frac{\mu^2}{g}\cdot I\left(H\frac{\mu^2}{g}\right)H\right]}\cdot\sin\left[\frac{\mu^2}{g} I\left(H\frac{\mu^2}{g}\right)\left[x\cos\theta + y\sin\theta\right] - \mu t + \psi(\mu,\theta)\right]\cdot\sqrt{\frac{g^2}{\mu^2}\left[A_{2H}(\mu,\theta)\right]^2 d\mu\, d\theta} \tag{12.17}$$

Plate LXII

have the same properties as required in Chapter 9 for the analogous functions in that chapter. The subscript H's have been added to emphasize the fact that, given $[E_2(\mu,\theta)]$ offshore in deep water, then $E_{2H}(\mu,\theta)$ is an unknown function unless the refraction properties of the transition zone are given.

The potential function is given by equation (12.17). $[A_{2H}(\mu,\theta)]^2$ is the power spectrum of the waves in water of depth, H. It cannot be found from the theories given in Chapter 10, although appropriate modifications of the formulas given therein would yield correct results.

As a function of time at a fixed point, these equations can be treated just as in Chapter 10. The record as a function of time is Gaussian and the results of Chapter 7 again apply. $E_{2H}(\mu)$ is by analogy equal to $E_{2H}(\mu,\pi/2)$. As before, $[A_H(\mu)]^2$ is the integral over θ of $[A_{2H}(\mu,\theta)]^2$.

The pressure at a depth, z, produced by a short crested Gaussian sea surface on the surface of a layer of water of depth, H, is given by equation (12.18). It reduces to the results given in Chapter 11 as the depth approaches infinity.

The pressure at a fixed point in the x,y plane as a function of z and t is given by equation (12.19). The equation can be derived by the use of the methods of Chapter 10. For a fixed value of z, a pressure record as a function of time is therefore Gaussian and can be analyzed for its pressure power spectrum in the same way that a wave record can be analyzed.

The power spectrum of the pressure record for a pressure recorder at any depth (not necessarily the bottom) is related to the

Pressure Records in Water of Constant Depth

$$p(x,y,z,t) = \rho g \int_0^{\infty} \int_{-\frac{\pi}{2}}^{\frac{\pi}{2}} \frac{\cosh\left[\frac{\mu^2}{g} I(H\frac{\mu^2}{g})\cdot(H+Z)\right]}{\cosh\left[\frac{\mu^2}{g} I(H\frac{\mu^2}{g})\cdot H\right]} \cdot \cos\left[\frac{\mu^2}{g} I(H\frac{\mu^2}{g})\left[x\cos\theta + y\sin\theta\right] - \mu t + \psi(\mu,\theta)\right] \cdot \sqrt{\left[A_{2H}(\mu,\theta)\right]^2 d\mu\, d\theta} \; - g\rho z \tag{12.18}$$

$$p(z,t) = \rho g \int_0^{\infty} \cos\left[\mu t + \psi'(\mu)\right] \sqrt{\left[\frac{\cosh\left[\frac{\mu^2}{g} I(H\frac{\mu^2}{g})(H+Z)\right]}{\cosh\left[\frac{\mu^2}{g} I(H\frac{\mu^2}{g})\cdot H\right]}\right]^2 \cdot \left[A_{2H}(\mu)\right]^2 d\mu} \; - g\rho z \tag{12.19}$$

$$\left[A_{pH}(\mu)\right]^2 = \left[\frac{\cosh\left[\frac{\mu^2}{g} I\left[H\frac{\mu^2}{g}\right]\cdot(H+Z)\right]}{\cosh\left[\frac{\mu^2}{g} I\left[H\frac{\mu^2}{g}\right]\cdot H\right]}\right]^2 \left[A_H(\mu)\right]^2 \tag{12.20}$$

at bottom ($z = -H$)

$$\left[A_{pH}(\mu)\right]^2 = \frac{\left[A_H(\mu)\right]^2}{\left[\cosh\left[\frac{\mu^2}{g} I(H\frac{\mu^2}{g})\cdot H\right]\right]^2} \tag{12.21}$$

$$p(-H,t) = \rho g \int_0^{\infty} \cos\left[\mu t + \psi'(\mu)\right] \sqrt{\frac{\left[A_H(\mu)\right]^2}{\left[\cosh\left[\frac{\mu^2}{g} I(H\frac{\mu^2}{g})\cdot H\right]\right]^2} d\mu} \; + g\rho H \tag{12.22}$$

Plate IXIII

power spectrum of the wave record taken of the free surface by equation (12.20). Given either one and given the depth of the water, and the depth of the instrument, the other can be computed except for the high spectral components lost by filtering due to depth due to the fact that the pressure recorder simply will not respond to minute variations in the pressure field.

At the bottom, z equals minus H, and equation (12.20) becomes equation (12.21). The pressure record recorded by a pressure recorder on the bottom is therefore some segment of one of the infinitely long records which result from the limit of a partial sum such as those discussed in Chapter 7.

Wave refraction in the transition zone

The refraction of the short crested Gaussian waves which have been derived in the previous chapters is an extremely complicated problem. The basic theory which has been derived by Sverdrup and Munk [1944], Johnson, O'Brien, and Isaacs [1948], Arthur [1946], Eckart [1951], and Arthur, Munk and Isaacs [1952], is correct, but it applies only to one pure sine wave of constant period. The theory needs to be placed upon a somewhat firmer theoretical basis as pointed out by Pierson [1951a], and the results of Eckart [1951] are a first step in this direction.

The theory of wave refraction is at the level of theoretical development which was attained by the theory of optics before the work of Luneberg [1944, 1947] in optics. That is, wave refraction theory has been derived not from the basic hydrodynamic equations, but by a series of approximations and assumptions about the nature of the motion of a pure sine wave over a bottom of variable depth.

For example, Snell's Law is either assumed or proved from very simple considerations. Also the shrinking in the wave length as the wave progresses into shallower water is not shown to be a continuous process; that is, the length in deep water is L_o, and the length in water of depth, H, is given by equation (12.10), but nowhere in the theory is the exact profile along an orthogonal given.

Luneberg started with Maxwell's equations and showed how the theory of geometrical optics for light or any other form of electromagnetic radiation could be derived rigorously from the equations. In addition, the systematic approach which he used has permitted attempts to refine the theory to the level of physical optics. Considerable success along these lines has been obtained by Keller, Kline, and Friedman of New York University.*

Similarly, it ought to be possible to derive wave refraction theory with the original hydrodynamic equations as a start. Were this done, the results would possibly indicate better relations for the wave height in the neighborhood of a caustic made possible by the consideration of higher order effects.

One fundamental assumption of wave refraction theory is that the dimensions of the refracting bottom contour systems must be large compared to the wave length of the waves on the surface. As has been pointed out by Pierson [1951a], in many practical cases

---

*The author in this section is indebted to Professor Joseph Keller for his series of lectures on geometrical optics given at the Math Institute during the past year. Wave refraction theory for Gaussian waves has an analogue in the problem of colored light scattered in two dimensions passing through a medium with a continuously varying index of refraction such that the index of refraction is a function of the wave length of the light and of only two space variables.

this assumption is not fulfilled too well. Thus some numerical results of wave refraction theory must not be taken too quantitatively although they may be correct within 30 or 40 per cent. Were the theory derived rigorously, it might then be possible to estimate the amount of error introduced by the above assumption in a practical case.

The refraction of a short crested Gaussian sea surface

From the results of the past chapters, it is possible to determine the two dimensional power spectrum at a point located offshore in deep water from a point of interest in the refraction zone. For example, the power spectrum could be determined by direct measurement from stereo-aerial photographs and deep water wave records as a function of time at a point a few miles from the coast under investigation. By the methods of Chapter 9, if the storm power spectrum were known, it would then be possible to forecast the power spectrum offshore from the point of interest. Given these deep water quantities, what can be said about the records which can be obtained in the transition zone?

The problem can be solved to various degrees of accuracy. Given a linear sloping beach, and the results obtained by Peters* expressed in terms of the parameters, μ and Θ, and a deep water wave of unit height, then it would be possible to find a representation for the sea surface in the transition zone by a Lebesgue Power Integral in the Gaussian case over the power spectrum multiplied by Peters' solution. At any point the wave record as a function of time would be Gaussian. As a function of x and y, the elemental

* See references to Part I. The paper has appeared in the publication cited.

crests would be curves in the refraction zone. Such a solution would be exact (in a linear sense) everywhere, and would agree well with reality until non-linear effects near the breaker zone caused it to fail. Apart from the difficulty of evaluating the result, (and it is difficult enough for a pure sine wave), very few linear sloping beaches are found in nature. As soon as the depth becomes a complicated function, wave refraction theory must be used.

The solution to the wave refraction problem in the transition zone is found in practice by graphical methods. The orthogonal method as presented by Johnson, O'Brien, and Isaacs [1948] and most recently by Arthur, Munk and Isaacs [1952]* is the best procedure because errors are not cumulative and the method discovers caustic curves. It would now appear that it is possible at a sufficient distance beyond the caustic to use the usual formulas for the value of $K_H D$ based on the separation of the orthogonals at the point of interest, if the wave is purely sinusoidal in deep water.

In general, for a pure sine wave in deep water, the crests in the transition zone are curved. All of the systems discussed so far consist of elemental straight crests. The equations for the crests in the transition zone are very complicated and they have rarely been formulated mathematically except for extremely simple bottom configurations. Some examples in which the crests can be found explicitly (since the orthogonals are given) can be found in papers written by Arthur [1946], Pierson [1951a] and Pocinki [1950].

* The abstract of the paper by Arthur, Munk and Isaacs[1952] can be found in the American Geophysical Union's program for its May 5-7, 1952 meetings in Washington. A preliminary copy provided by the authors shows that errors in previous methods can be eliminated by a more refined application of Snell's law.

In general, the refraction problem is treated even less specifically for practical purposes. Given the deep water wave direction, amplitude and period of a pure sine wave, data are usually provided which give the angle the crest makes with the shore and the amplitude of the sine wave as observed at one point of special interest. For example, the data presented by Pierson [1951a] for Long Branch apply only to one point, namely the point where the wave recorder used to be. It was at a depth of 21 feet, mean low water, offshore from latitude 40°18.2'. It is now at a depth of 30.5 feet, mean low water, offshore from latitude 40°18.2'. The slight change in location has negligible effects for this case since most of the refraction occurs in deeper water.

In figure 32, consider the point B, in deep water just outside of the transition zone. At the point B, x_D and y_D are zero and the wave system will be referred to the Cartesian coordinate system indicated on the figure. If a pure sine wave of spectral frequency, μ_I, were to exist in deep water and if it were traveling in the direction, θ_F^* (measured with respect to θ_F^* equal to zero coincident with the x_D axis), then the sea surface could be given by equation (12.23). The equation would hold everywhere in deep water. In the transition zone, equation (12.23) is not valid.

In figure 32, consider the point C in the transition zone. At the point C, x_R and y_R are zero. The x_R axis is parallel to the x_D axis (and not necessarily coincidental). The depth at that point is $H(x_R,y_R) = H = H(0,0)$ referred to this coordinate system. If the assumptions of wave refraction theory hold, then the bottom is nearly level at that point. The crests although slightly curved will have

The Transition Zone

In Deep Water near $x = x_D$, $y = y_D$

$$\eta = A \cos\left[\frac{\mu_I^2}{g}\left[x_D \cos\theta_F^* + y_D \sin\theta_F^*\right] - \mu_I t\right] \tag{12.23}$$

In Transition Zone, near $x = x_R$, $y = y_R$

$$\eta = A_{RH} \cos\left[\frac{\mu_I^2}{g} I\left(\frac{\mu_I^2}{g}H\right)\left[x_R \cos\theta_R + y_R \sin\theta_R\right] - \mu_I t + \delta\right] \tag{12.24}$$

where $A_{RH} = K_H D\, A$ (12.25)

Problem; to generalize above to a short crested Gaussian Sea Surface

Definitions of Terms

$\left[A_2(\mu,\theta)\right]^2$ is the power spectrum at the edge of the fetch (12.26)

$\left[A_{2F}(\mu,\theta_F)\right]^2$ is the forecasted power spectrum at the point offshore from point of forecast given by x_D, y_D. (12.27)

$\theta_F = \theta - \theta_D$ from equation (9.61) (12.28)

$\left[A_{2F}^*(\mu,\theta_F^*)\right]$ is the forecasted power spectrum at the point x_D, y_D rotated to line it up with the refraction diagram (12.29)

$\theta_F^* = \theta_F - \beta$ where β is the angle between the continuation of R through B and the line drawn out to sea perpendicular to the coast through the point (x_R, y_R) (12.30)

$\left[A_{2RH}(\mu,\theta_R)\right]^2$ is the forecasted power spectrum in the Refraction Zone at the point x_R, y_R and at the depth, H (12.31)

Problem; To find $\left[A_{2RH}(\mu,\theta_R)\right]^2$ from refraction diagram data and the forecasted power spectrum.

Plate LXIV

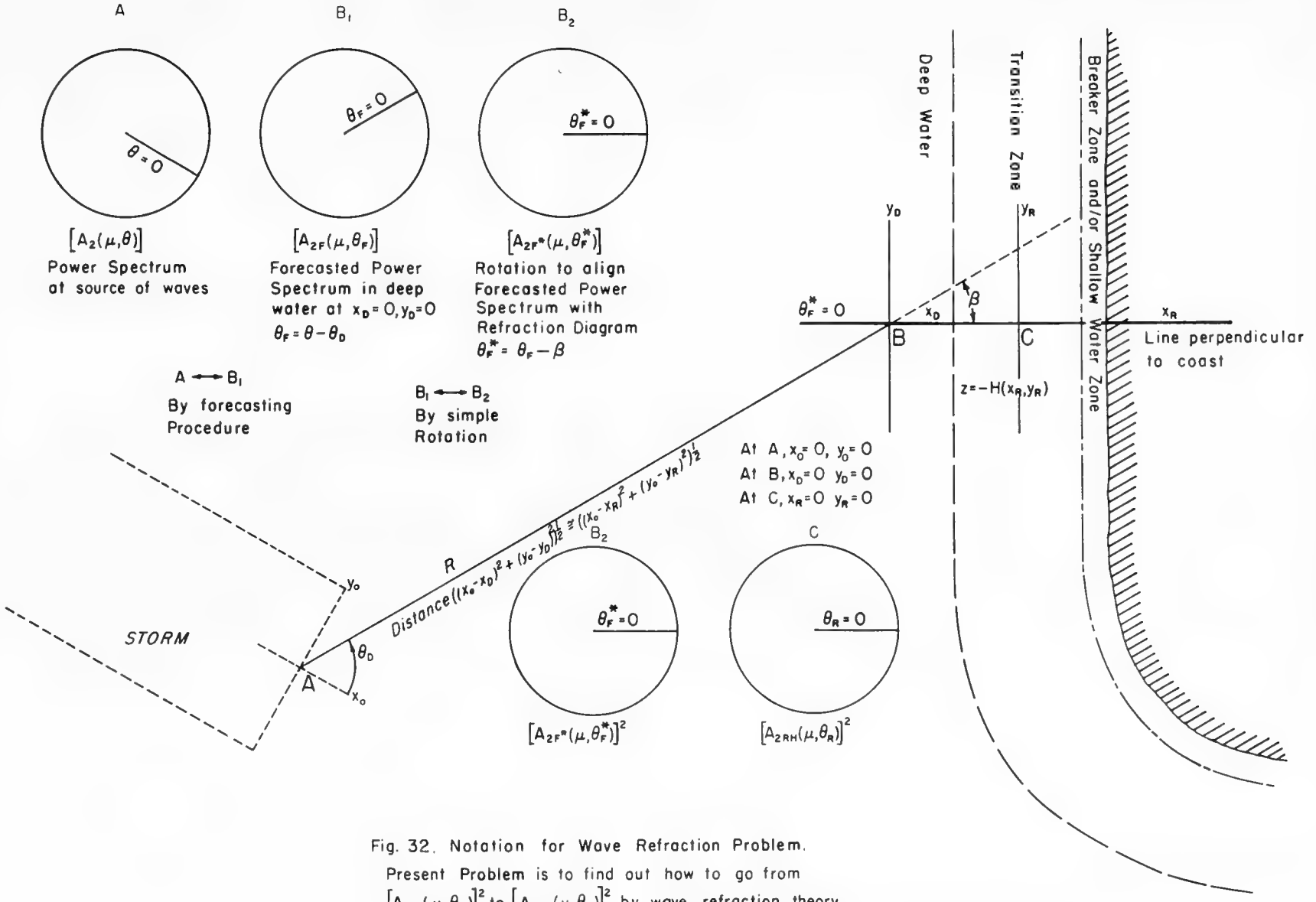

Fig. 32. Notation for Wave Refraction Problem.
Present Problem is to find out how to go from $\left[A_{2F}(\mu,\theta_F)\right]^2$ to $\left[A_{2RH}(\mu,\theta_R)\right]^2$ by wave refraction theory.

a certain direction of forward progress at the point and a wave length determined by μ_I and H. Finally, the crests will have a new amplitude and phase at that point, which can be determined from tracing the family of orthogonals near the point of study. These features are all incorporated in equation (12.24). A_{RH} is the new height at the new point of observation which can be determined from A by wave refraction theory and equation (12.25). θ_R is the new direction of progress of the crests. δ is a phase lag due to the slowing down of the crests.

Equation (12.24) does not hold everywhere in the transition zone. In fact it holds only at one point; namely, $x_R = 0$, $y_R = 0$. However, in the vicinity of the point, the equation approximates the local state of affairs. The degree of approximation is somewhat crude but actually to develop the formulas with curved crests which would apply to greater distances away from the point of observation would be far too difficult.

The problem of the refraction of a short crested Gaussian sea surface can be solved by showing how it is possible to extend the application of the refraction data already obtained for pure sine waves to an infinite sum of infinitessimally high sine waves in random phase. It can be done easily to the degree of approximation just described above. In this way, the sea surface is approximated in the vicinity of the point under study by a Lebesgue Power Integral quite similar to the one discussed above and in previous chapters. A wave record taken as a function of time at the point of interest will be quite accurately given but the slight curvature of the individual crests in the neighborhood of x_R, y_R will not be represented.

From the edge of the fetch to the transition zone

At the edge of a storm at sea, in connection with the forecasting problem, it is more convenient to line up the θ equal to zero axis with the direction of the winds in the storm. The distance R, from the center of the forward edge of the storm to the edge of the transition zone is essentially the same, as far as the magnitude of the parameters is concerned, as the distance to the point, $x_R = y_R = 0$ in the transition zone. Thus in figure 32, the distance from A to B is essentially the same as the distance from A to C. In the process of forecasting considerations for the point, C, then, the procedures presented in Chapter 9 can be applied to reach the point, B, and then refraction theory can be applied without consideration of the added distance from B to C in order to find the effects at C. This procedure also neglects some minor effects on the power spectrum since it varies slowly from point to point in deep water and all rays arriving at C do not come from B. Various operations must be applied to the power spectrum at the source in order to find the power spectrum at B and in order to put it into a mathematical form which permits the application of refraction theory to the power spectrum at B. Then the problem of prime importance in this chapter is to show how it is possible to go from the point B to the point C.

The operations needed to proceed from point A to B and to orient the forecasted spectrum at B so that it can be easily refracted are shown on the right of figure 32. The various terms are defined in Plate LXIV.

At the forward edge of the storm, the power spectrum can be

defined to be $[A_2(\mu,\theta)]^2$ as in equation (12.26). The angle θ is defined as zero along the x axis defined in relation to the storm in connection with the forecasting problem. At B, the forecasted power spectrum can be found from the results of Chapter 9. A new angular variable can then be found, which will be called θ_F. In terms of the forecasted power spectrum, by equation (12.28), the power spectrum at B is given by $[A_{2F}(\mu,\theta_F)]^2$. The direction θ_F equals zero is usually the dominant apparent direction of the short crested waves at B. The line, θ_F equal to zero, is shown on the coordinate system labeled B, in figure 32.

The variable, θ_F, must be transformed to the variable, θ_F^*, in order to align the forecasted power spectrum with the refraction diagrams for the point C. The angle, θ_F^*, can best be picked to be zero when the angle coincides with the x_D axis chosen perpendicular to the coast through the point C. The angle β, which defines θ_F^* in terms of θ_F is the angle between the continuation of R through B and the line x_R equal to zero. The function $[A_{2F}^*(\mu,\theta_F^*)]^2$, is thus the forecasted power spectrum at B aligned properly to the $x_R = 0$ and $x_D = 0$ axis. The line, θ_F^* equal to zero, is shown on the polar diagram marked B_2 in figure 32.

If now, $[A_{2RH}(\mu,\theta_R)]^2$ is defined to be the power spectrum at the point, C, (that is, in the vicinity of the point $x_R = 0$, $y_R = 0$), how can it be determined from $[A_{2F}^*(\mu,\theta_F^*)]^2$ given the usual refraction data? It can be found by applying operations to the continuous spectrum which are analogous to those operations applied to pure sine waves in the theory of wave refraction. The reader can check each step of what follows and assure himself that each step applied to a sum such as in equation (8.5) would yield correct results for each discrete component.

Needed modifications of refraction diagrams

The next step is to modify the usual refraction data so that they can be easily applied to $[A_{2F}^*(\mu, \theta_F^*)]^2$. One of the quantities evaluated in a study of refraction is the quantity K_H. This quantity is a value related to the ratio of the distance between orthogonals at the point of observation to the distance between the same orthogonals in deep water. Procedures for obtaining the quantity are given by Johnson, O'Brien, and Isaacs [1948]. The value of K_H must be multiplied by a factor D which depends on the depth below the point of observation and the period of the wave. It is essentially a correction for the group velocity effect in order to maintain a constant energy flux between orthogonals. The product $K_H D$ is usually then plotted as a function of the period and deep water direction of the wave. Such diagrams are given by Munk and Traylor [1947] and Pierson [1949]. The isopleths are lines of constant $K_H D$ on a polar diagram. To prepare such a diagram for application to the refraction of a Gaussian short crested wave system, it is necessary to invert the diagram and plot it as a function of μ and θ_F^* where μ is the spectral frequency and θ_F^* is the direction toward which an elemental crest is moving just offshore in deep water (θ_F^* is zero when the crest in deep water is parallel to the coast). The values on the diagram must also be squared point for point. The result is a considerably more rapidly varying function which will be defined to be the function $[K_H D(\mu, \theta_F^*)]^2$ as in equation (12.32) and which will be named the spectrum amplification function. The function must approach unit values as μ approaches values of the spectral frequency such that the depth is greater than one half of $2\pi g/\mu^2$.

The other quantity usually evaluated in refraction data is the angle the crests make with the shore at the point of observation near the shore. This angle is identically equal to θ_R which is the direction toward which the elemental crest is traveling. θ_R equal to zero designates a crest traveling directly toward the coast. These values can be plotted as a function of μ and θ_F. The function, $\theta_R = \Theta(\mu, \theta_F^*)$, can thus be shown as isopleths of θ_R as a function of μ and θ_F^*. As μ becomes large, θ_R equals θ_F^* asymptotically. These relations are defined in equation (12.33). $\Theta(\mu, \theta_F^*)$ will be called the direction function.

The inverse of $\theta_R = \Theta(\mu, \theta_F^*)$ is also needed. That is, values of θ_F isoplethed on a μ, θ_R polar coordinate system, are needed. This inverse function is defined by equation (12.34) as $\theta_F^* = \Theta^*(\mu, \theta_R)$.

From the isoplethed values of equation (12.34) it is possible to evaluate $\Gamma(\mu, \theta_R)$ as given by equation (12.35). The function, $\Gamma(\mu, \theta_R)$, is the change of θ_F^* per unit of change of θ_R expressed as a dimensionless number in radians per radian or degrees per degree. $\Gamma(\mu, \theta_R)$ is a measure of the crowding together of the power spectrum due to refraction and its significance will be discussed later. It is the Jacobian of the inverse of the direction function.

Steps in wave refraction

Given the functions described above and their definitions, three steps are required to find $[A_{2RH}(\mu, \theta_R)]^2$ from $[A_{2F}^*(\mu, \theta_F^*)]^2$. The function, $[A_{2F}^*(\mu, \theta_F^*)]^2$, could also be the power spectrum of any system observed immediately offshore in deep water. At this stage, then, the functions defined by equations (12.29), (12.32), (12.33), (12.34) and (12.35) are known.

The Transition Zone

$\left[K_H D(\mu,\theta_F^*)\right]^2$ is the spectrum amplification function. It is the square of the ordinary Refraction Diagram plotted in the μ,θ_F^* plane instead of in the T,θ plane. (12.32)

$\theta_R = \Theta(\mu,\theta_F^*)$ is the angle that the crest makes with the y axis at y_R, x_R plotted as a function of μ and θ_F^*, i.e. the wave frequency and the deep water direction with respect to a line perpendicular to the coast at the forecast point. (12.33)

$\theta_F^* = \Theta^*(\mu,\theta_R)$ is the inverse of the function given above (12.34)

$$\frac{\partial\theta_F^*}{\partial\theta_R} = \frac{\partial\Theta^*(\mu,\theta_R)}{\partial\theta_R} = \Gamma(\mu,\theta_R) \qquad (12.35)$$

Steps in Wave Refraction

Step I; Multiply $\left[A_{2F}^*(\mu,\theta_F^*)\right]^2$ by $\left[K_H D(\mu,\theta_F^*)\right]^2$ graphically to find

$$\left[A_{2F}^*(\mu,\theta_F^*)\right]^2 \cdot \left[K_H D(\mu,\theta_F^*)\right]^2 \qquad (12.36)$$

Step II; Substitute equation (12.34) for θ_F^* to express (12.36) as a function of θ_R and find $\left[A_{2F}^*(\mu,\Theta^*(\mu,\theta_R))\right]^2 \cdot \left[K_H D(\mu,\Theta^*(\mu,\theta_R))\right]^2$ (12.37)

Step III Correct, by multiplication by equation (12.35), for distortion to find $\left[A_{2RH}(\mu,\theta_R)\right]^2 = \left[A_{2F}^*(\mu,\Theta^*(\mu,\theta_R))\right]^2 \left[K_H D(\mu,\Theta^*(\mu,\theta_R))\right]^2 \Gamma(\mu,\theta_R)$ (12.38)

Plate LXV

Step one is to multiply the power spectrum in deep water by the spectrum amplification function. Graphically this can be done by computing the value of the product point for point of (12.29) and (12.32). For any finite net over $[A_{2F}{}^*(\mu,\theta_F{}^*)]^2$, as in equation (9.22), the result of this operation is to predict the height of each elemental wave in the partial sum for the new point of observation.

Step two is to substitute equation (12.34) for $\theta_F{}^*$ everywhere it occurs. This converts the product given in (12.36) to the product given in (12.37). The result is some function of μ and θ_R. For any partial sum the result is to assign the correct spectral directions to each elemental wave at the new point of observation. In general equation (12.36), is a continuous function and the effect of this operation is to squeeze (12.36) into a more compact function in the μ ,θ_R plane since elemental wave components with widely different directions in deep water have more nearly the same direction at the point of observation in the transition zone.

Graphically this step can be accomplished by plotting the value of (12.36) at $\mu = \mu_I$ and $\theta_F{}^* = \theta_{FI}^*$ in the μ ,$\theta_F{}^*$ coordinate system at the point $\theta_R = \Theta(\mu_I\theta_{FI}^*)$ and $\mu = \mu_I$ in the new μ ,θ_R polar coordinate system. A line on which (12.36) is a constant is thus mapped into a new line in the μ ,θ_R plane on which the same constant value is found.

The third step is to multiply (12.37) by $\Gamma(\mu,\theta_R)$ as given by equation (12.35). The result is the desired power spectrum, $[A_{2RH}(\mu,\theta_R)]^2$, as a function of μ and θ_R at the point of observation in the transition zone. This step is needed since the power

spectrum is treated as a continuous function. If the spectrum were discrete jumps in $E_2(\mu,\theta)$ as in equations (9.38b) and (9.39), this step would not be needed.

$\Gamma(\mu,\theta)$ could be called the distortion correction function. It is the Jacobian or equation (12.34) and it corrects for the squeezing together of (12.36) when it is changed to (12.37).

Consider an example to clarify this point. Suppose that (12.36) is given by a constant value from μ equal to $2\pi/10$ to μ equal to $2\pi/9$ and for θ_F^* equal to $-\pi/30$ to $+\pi/30$ and by zero otherwise, and that (12.37) is the same except that θ_R ranges from $-\pi/60$ to $+\pi/60$. Both (12.36) and (12.37) represent the average potential energy at the new point of observation, and yet the integral over μ and θ_F^* for the first case is <u>not</u> equal to the integral over μ and θ_R in the second case. But the value of $\partial\theta_F^*/\partial\theta_R$ in this case is equal to two radians per radian, and thus doubling the value of the second spectrum corrects the value of the average potential energy.

The power spectrum of the waves in the vicinity of the point under study in the transition zone is now known. It is given by equation (12.38). In terms of the x_R, y_R coordinate system at the point, C, in figure 32, and in terms of the μ, θ_R, power spectrum defined there by the above procedures, the short crested sea surface near x_R and y_R equal to zero is given by equation (12.39). In appearance, the sea surface will be different in many ways from the sea surface at the point, B. The procedures described above predict many properties of the waves at the point C which are verifiable by aerial photographs and observational procedures. The properties will be described later.

One property which follows from the derivation is given by

The Transition Zone

Given $\left[A_{2F}^{*}(\mu,\theta_F^{*})\right]^2$ and needed refraction diagram and other data

$$\eta(x_R,y_R,t) = \int_0^{\infty}\int_{-\pi}^{\pi} \cos\left[\frac{\mu^2}{g} I\left(\frac{\mu^2 H}{g}\right)\left[x_R\cos\theta_R + y_R\sin\theta_R\right] - \mu t + \psi(\mu,\theta_R)\right]\sqrt{\left[A_{2RH}(\mu,\theta_R)\right]^2 d\theta\, d\mu} \tag{12.39}$$

$$\int_0^{\infty}\int_{-\pi}^{\pi}\left[A_{2F}^{*}(\mu,\theta_F^{*})\right]\left[K_H D(\mu,\theta_F^{*})\right]^2 d\theta_F^{*} d\mu = \int_0^{\infty}\int_{-\pi}^{\pi}\left[A_{2F}^{*}(\mu,\theta^{*}(\mu,\theta_R))\right]^2\left[K_H D(\mu,\theta^{*}(\mu,\theta_R))\right]^2 \Gamma(\mu,\theta_R) d\theta_R\, d\mu$$

$$= \int_0^{\infty}\int_{-\pi}^{\pi}\left[A_{2RH}(\mu,\theta_R)\right]^2 d\theta_R\, d\mu \neq \int_0^{\infty}\int_{-\pi}^{\pi}\left[A_{2F}^{*}(\mu,\theta_F^{*})\right]^2 d\theta_F^{*} d\mu \tag{12.40}$$

$$\eta(t) = \int_0^{\infty}\cos(\mu t + \psi'(\mu))\sqrt{\left[A_{RH}(\mu)\right]^2 d\mu} \tag{12.41}$$

$$P(-H,t) = \rho g \int_0^{\infty}\cos(\mu t + \psi'(\mu))\sqrt{\frac{\left[A_{RH}(\mu)\right]^2}{\left[\cosh\left[\frac{\mu^2}{g} I\left(\frac{H\mu^2}{g}\right)H\right]\right]^2}}\, d\mu + g\rho H \tag{12.42}$$

The power spectrum of the function observed by most pressure recorders

$$\left[A_{RPH}(\mu)\right]^2 = \frac{\left[A_{RH}(\mu)\right]^2}{\left[\cosh\left[\frac{\mu^2}{g} I\left(\frac{H\mu^2}{g}\right)H\right]\right]^2} \tag{12.43}$$

Plate LXVI

equation (12.40). After multiplication of the deep water power spectrum by the spectrum amplification function, (12.32), the subsequent change of variables does not affect the potential energy of the waves at the point of observation. Nevertheless the potential energy at the point in the transition zone may be completely different from the potential energy in deep water since the spectrum amplification function in general does not leave the total volume under $[A_{2F}^{*}(\mu, \theta_F^{*})]^2$ unaltered.

The spectrum amplification function can change markedly upon the choice of different points, C, in the transition zone. In the short distance of thirty miles along the coast of New Jersey, it can vary tremendously. Consequently not only will the wave height vary over a distance in the transition zone which is very short compared to the deep water forecast parameters but also the "significant" period will vary from place to place. These points will be verified by examples in a later chapter.

The wave record at the point of observation

The wave record which will be observed by, say, a step resistance guage at the point $x_R = 0$, $y_R = 0$ is given by equation (12.41) where $[A_{RH}(\mu)]^2$ is the integral over θ_R of $[A_{2RH}(\mu, \theta_R)]^2$. This function has all of the properties of the one described in Chapter 7 and it can be derived from equation (12.37) by the exact same arguments given in Chapter 10 for the deep water case. In Chapter 7, a wave record in the transition zone was shown to have the property that points chosen at random from it were normally distributed. The definition of the integral given in equation (7.1) and in subsequent equations can just as easily be applied to equation (12.41)

and the results are thus to be expected. The reader, though, would have been perfectly justified in objecting at that point in Chapter 7 where a transition zone wave record and transition zone pressure records were used to prove the Gaussian property, and then the Gaussian property was tacitly assumed for deep water waves. These results now show that given that the waves have the Gaussian property in deep water, it then follows that they have the Gaussian property in the transition zone (and conversely since the wave refraction process can be theoretically reversed).

From equations (11.3), (12.41), (12.18), and (12.21), it then follows that the pressure record which will be recorded at the bottom by a pressure guage at the point of observation in the transition zone is given by equation (12.42). The pressure record is therefore Gaussian. The power spectrum of the pressure record is related to the power spectrum of the waves passing overhead by equation (12.43). Given $[A_{RPH}(\mu)]^2$, the power spectrum for the surface record can be computed from equation (12.43), and conversely. For those pressure recorders which respond to different periods in different ways, the calibration curve appropriately modified must be inserted as another function at this point. An instrument with a completely flat response curve is assumed in this derivation.

Ewing and Press [1949] are of course correct in their statement of the problem of pressure record analysis. These formulas simply formalize the procedures to be employed.

Equations (12.42) and (12.43) are extremely important to the practical engineer. Nearly all of the wave records being taken at the present time in the United States are made with a pressure recorder

on the bottom at a point in the transition zone at some depth, H. The techniques currently employed in the analysis of these records, for example as summarized most recently by Snodgrass [1951], are for all practical purposes useless. For that matter any step in current practices which involves the assumption that the "significant" period can be treated as if it were a discrete spectral component automatically introduces huge errors for "sea" records which completely invalidate all quantitative values which result from the analysis.

In order to demonstrate this point, some statements will be quoted from the paper by Snodgrass [1951]. Then the point at which the error was made will be shown. Finally Snodgrass' analysis of the inaccuracies which result will be interpreted in the light of the results shown in this chapter. Selected quotations from the paper referred to above follow.

> ....."The following basic definitions have been accepted (Folsom, 1949):
>
> 1.....
>
> 2.....
>
> 3. Wave period is the time interval between the appearance at a fixed point of successive wave crests.
>
> 4. Characteristic wave period is the average period for the well-defined series of highest waves observed.
>
> .....
>
> "Analysis of wave records for wave period. Analysis of wave records for the characteristic period is accomplished by measuring the average period of the larger, well-defined waves appearing on the record..... The characteristic period of the waves does not describe the period-distribution, as the characteristic height describes wave-height distribution. ..... Additional information is needed to adequately describe wave periods.
>
> .....

"Analysis of under-water pressure records. The analysis of pressure records for wave period is the same as the analysis of surface wave records. The records differ, however, in that the short period waves are not registered to the same degree as the long period waves by pressure recorders due to the hydrodynamic pressure attenuation of the water. As a result, many of the shorter period waves may not appear on the pressure record.

"If the technique of measuring the periods of only the larger, well-defined waves of the record is followed (as described in the above section), the measured period will be approximately the same as would be obtained if the record were made with a surface type gage. For locations on the exposed coast, the short period waves, not recorded by pressure, generally are generated by local wind. Irregular and of small amplitude, these waves are neglected in the analysis of surface records.

"In several cases, attempts have been made to utilize the hydrodynamic attenuation of short period waves by installing gages in deep water (about 600 feet) so that only the waves of long periods (the characteristic forerunners of storms) will be recorded. These long period waves are recorded by pressure heads installed in shallow water, but are "lost" in the record of shorter period waves. Installations of this type of instrument have been made, but due to instrument difficulties no satisfactory records have been obtained.

"To obtain the surface wave heights from the pressure record, two factors are required; (1) the calibration of the instrument and (2) the pressure response factor relating the subsurface pressure fluctuations to the surface wave. Thus, if

H = wave height at the surface (in feet);

C_i = calibration factor of the instrument (expressed in feet of water pressure variation per chart division);

K = pressure response factor based on the depth of the instrument, the depth of the water and the length (or period) of the wave being recorded;

R_i = reading of the instrument;

the following equation is used to obtain the surface wave height:

$$H = C_i/K\ (R_i) \quad . \quad . \quad . \quad . \quad . \quad . \quad . \quad . \quad . \quad . \quad . \quad . \quad (1)$$

"The calibration factor for most instruments in use today is a constant independent of wave period and depth of the instrument. The instrument provides a record of the pressure variations at the instrument which is accurate in amplitude and wave form.

"The relation of the subsurface pressure fluctuations to the surface wave has been determined theoretically for two dimensional, irrotational motion of an incompressible fluid in a relatively deep channel of constant depth (Folsom, 1947). The response factor K has been shown to be:

$$K = \frac{\cosh 2\pi d/L\ (1 - z/d)}{\cosh 2\pi d/L} \quad \ldots\ldots\ldots\ldots \quad (2a)$$

where

z = depth at which the pressure variation is being measured (in feet),

d = depth of water at the instrument (in feet),

L = length of the surface wave (in feet).

"When z = d, the pressure variation is measured at the bottom and equation 2a reduces to:

$$K = \frac{1}{\cosh 2\pi\ d/L} \quad \ldots\ldots\ldots\ldots \quad (2b)$$

Pressure records do not enable the direct measurement of wave length; the wave length must be calculated from the wave period using the following equation:

$$L = \left(\frac{gT^2}{2\pi}\right) \tanh 2\pi\ d/L \quad \ldots\ldots\ldots\ldots \quad (3)$$

Where T = wave period (in seconds).

" Suitable graphs and tables (Wiegel, 1948) are available for the solution of these equations. Graphs have been prepared which enable the response factor (K) to be determined if the water depth (d), instrument depth (z) and wave period (T) are known. Two errors arise when the above equations are used to determine the response factor (K) for ocean waves; (1) an average or characteristic period must be used in the equation while the actual wave period is continuously varying and individual waves are not sinusoidal in form, (2) wave heights computed from these equations have been shown by several observers to be from six to twenty-five percent too low.

"Considering the first of these two errors, greater accuracy probably could be attained if the pressure response factor (K) were determined for each wave and the equivalent surface wave were individually computed. This procedure might be feasible from a practical standpoint if the statistical distribution of wave height and wave period could be established so that fewer waves need to be analyzed to completely describe the state of the waves. (See the above section on "Analysis of wave records for wave height".)

"The second of these two errors emphasizes the need to reconsider the basic theory which does not agree with experiment. Every observer who has simultaneously measured the surface waves and the subsurface pressure fluctuations has found the theoretical response factor determined from equation 2a to be too small. Ten random measurements made at the Waterways Experiment Station (Folsom, 1947) indicated an average correction of 1.07 should be applied to equation 1. Seventeen laboratory measurements at the University of California, Berkeley, indicated an average correction of 1.10 (1949). Field data reported by the Woods Hole Oceanographic Institute (Admirality Research Laboratory, 1947; Seiwell, 1947) indicated a correction factor in excess of 1.20 while the three sets of field data obtained at the University of California (Folsom, 1946) indicated values of 1.06, 1.08, and 1.18."

- - -

The basic fallacy occurs at the very beginning of the material quoted when the statement is made that "The following basic definitons have been accepted" and that the "wave period is the time interval between the appearance at a fixed point of successive wave crests." What is measured are the time intervals between successive relative maxima of a non-periodic* function. These time intervals have absolutely nothing to do with the time intervals between successive crests of a pure sine wave such as in equation (2.19). From the measurement of this quantity, the error is compounded by averaging a number of such measured quantities and calling the result the "characteristic wave period." From then on, the "characteristic wave period" is applied to the wave record as if it were actually the true period of the wave record and as if the wave record had one discrete spectral component. All wave records are thus treated as if they were the one special case given in example one of Chapter 9. All of the subsequent formulas quoted are also based upon this assumption.

---

* See the correct mathematical definition of period in Chapter 2 (equation (2.11) for a pure sine wave).

For a "swell" record with a narrow band width such as those shown in Chapter 9, the fallacy of the method does not produce too important a discrepancy between the theoretically computed values of the surface quantities and the observed surface quantities, but for a "sea" record, such as those shown in the appendix to part one, the procedure effectively ignores a large part of the high end of the power spectrum. The surface "significant" height (or "characteristic" height) in "sea" conditions is always observed to be greater than the value predicted erroneously from the pressure record, and the surface "significant" period, (or "characteristic" period), were it also measured, would be found to be lower than the "significant" period (or the "characteristic" period) of the pressure record.

Thus the fact that "wave heights computed from these equations have been shown by several observers to be from six to twenty-five percent too low" is not at all surprising. The error is not a consistent error in that it varies from record to record depending on the power spectrum and in that it varies as a function of the depth of the pressure recorder. If the basic theory referred to in the last paragraph of the quotation is the theory which accepts as a basic definition the definition of wave period at the start of the quotation, then these considerations have shown wherein the error of the theory lies.

On the other hand, if the basic theory referred to in the last paragraph of the quotation is the theory of purely sinusoidal waves with one discrete period, then that basic theory is correct and the theory has been misapplied to a pressure record which is not a purely

sinusoidal variation with one discrete spectral period.

Finally, stated another way, most of the current theoretical work on wave theory would be correct if ocean waves were actually pure sine waves. Since ocean waves are not pure sine waves, the theory has been misapplied to situations it cannot possibly adequately describe. The derivations and considerations in this paper when they refer to Gaussian systems apply exactly to ocean waves as they actually are, except for non-linear effects. In a later chapter a pressure record will be correctly analyzed, and the correct values of the surface wave record will be deduced from the analysis by the use of equation (12.43).

To the reader, it may seem that the author is being unduly harsh with the authors of other works using the incorrect methods described above. The works of Wiener, Tukey, and Hamming did not appear until 1949, and the methods and techniques based on the significant height and period were undoubtedly the best that could be employed at the time. The literature on practical wave theory is full of such results, in particular, some of the results of Pierson [1951a] which use the concept of significant height and period to obtain theoretical results are completely wrong and practically useless.

The velocity field, kinetic energy, and energy flux in the transition zone

From previous considerations, the u, v, and w velocities at the point of observation are given by equations (12.44), (12.45), and (12.46). The vertical velocity is zero at the bottom, and the functions automatically satisfy the equation of continuity and consequently

the potential function. At z equal to zero the expressions simplify considerably, and possibly some interesting properties about the power spectra in the transition zone can be deduced by considerations similar to those of the previous chapter.

The kinetic energy integrated over depth and averaged over time and the y_R direction is given by equation (12.47). The Itcoth of $\mu\,{}^2H/g$ times the hyperbolic tangent of $\mu\,{}^2H/g[I(\mu,H)]$ is equal to one by virtue of equation (12.11). Thus the average kinetic energy is equal to the volume under $[A_{2RH}(\mu,\theta_R)]^2$ (that is, equation (12.48)) times $\rho g/4$. From previous considerations this is equal to the potential energy averaged over y_R and t. At a fixed point, say, x_R and y_R equal to zero, where the statement is exact these values also hold and the potential energy and the kinetic energy (integrated over depth) averaged over time are both equal to $(\rho g\, E_{RHmax})/4$. This statement can be proved by use of the results of Chapter 10.

The flux of energy toward shore in ergs/sec per centimeter of length along the y_R axis, is the average value of the work being done on the y_R,z plane determined by setting x_R equal to zero. The wave power is then given by equation (12.49), and the results check with the same result in Lamb [1932] where the flux is determined for a pure sine wave.

If the short crested wave system is concentrated in a narrow θ_R band width at the point of observation, and if the important spectral components are all traveling in nearly the same direction, say θ_{R1}, then it is possible to omit the cos θ_R term in equation (12.49). Then equation (12.49), as modified, is the flux of energy in the θ_{R1} direction at the point of observation. It can then be estimated (except for the short crested effect) from $[A_{RH}(\mu)]^2$ as

$$u = \int_0^{\infty}\int_{-\frac{\pi}{2}}^{\frac{\pi}{2}} \cos\left[\frac{\mu^2}{g} I(\mu,H)(x_R\cos\theta_R + y_R\sin\theta_R) - \mu t + \psi(\mu,\theta)\right] \cos\theta_R \sqrt{\left[\frac{\mu I(\mu,H)\cosh\left[\frac{\mu^2}{g} I(\mu,H)\cdot(z+H)\right]}{\cosh\left[\frac{\mu^2}{g} I(\mu,H)H\right]}\right]^2 \left[A_{2RH}(\mu,\theta_R)\right]^2}\, d\mu\, d\theta \tag{12.44}$$

$$v = \int_0^{\infty}\int_{-\frac{\pi}{2}}^{\frac{\pi}{2}} \cos\left[\frac{\mu^2}{g} I(\mu,H)(x_R\cos\theta_R + y_R\sin\theta_R) - \mu t + \psi(\mu,\theta)\right] \sin\theta_R \sqrt{\left[\frac{\mu I(\mu,H)\cosh\left[\frac{\mu^2}{g} I(\mu,H)\cdot(z+H)\right]}{\cosh\left[\frac{\mu^2}{g} I(\mu,H)H\right]}\right]^2 \left[A_{2RH}(\mu,\theta_R)\right]^2}\, d\mu\, d\theta \tag{12.45}$$

$$w = \int_0^{\infty}\int_{-\frac{\pi}{2}}^{\frac{\pi}{2}} \sin\left[\frac{\mu^2}{g} I(\mu,H)(x_R\cos\theta_R + y_R\sin\theta_R) - \mu t + \psi(\mu,\theta)\right] \cdot \sqrt{\left[\frac{\mu I(\mu,H)\sinh\left[\frac{\mu^2}{g} I(\mu,H)\cdot(z+H)\right]}{\cosh\left[\frac{\mu^2}{g} I(\mu,H)H\right]}\right]^2 \left[A_{2RH}(\mu,\theta_R)\right]^2}\, d\mu\, d\theta \tag{12.46}$$

$$\overline{\overline{KE}}^{yt} = \int_{-H}^{0} \overline{K.E.\, dz}^{yt} = \lim_{\substack{\bar{t}\to\infty \\ \bar{y}\to\infty}} \frac{1}{\bar{y}\,\bar{t}} \int_{y_R^*}^{y_R^*+\bar{y}} \int_{t^*}^{t^*+\bar{t}} \left[\int_{-H}^{0} \frac{\rho}{2}(u^2+v^2+w^2)\, dz\right] dt\, dy = \frac{\rho g}{4} I(\mu,H)\tanh\left(\frac{\mu^2}{g} I(\mu,H)H\right) E_{RHmax} = \frac{\rho g}{4} E_{RHmax} \tag{12.47}$$

where $$E_{RHmax} = \int_0^{\infty}\int_{-\frac{\pi}{2}}^{\frac{\pi}{2}} \left[A_{2RH}(\mu,\theta_R)\right]^2 d\theta_R\, d\mu \tag{12.48}$$

Plate LXVII

determined from either a pressure record and equation (12.43) or from a record of the free surface. The computation of the energy flux from the "significant" height and period is completely meaningless, especially for "sea" conditions.

If the beach has contours parallel to a straight shoreline, and if the waves have infinitely long crests (as in equation (7.36)) which are parallel to the shore, then the wave power integrated over depth and averaged over time is given by equation (12.50) on the left in the transition zone and on the right in deep water. The energy flux in this case only, is equal at both points. Equation (12.50) is the extension of usual refraction theory considerations to Gaussian systems. Equations (12.51) and (12.52) are the analogues to (12.50) for the discrete case. They are given by Sverdrup and Munk [1944b] and Mason [1951].

Additivity of power spectra*

One of the unsolved problems of wave forecasting and wave analysis theory in terms of "significant" height and period was the problem of the combination of wave systems from two different storms either in deep water or in the transition zone. In terms of power spectra and the methods developed in this paper, the problem can easily be solved. It is easy to prove that the power spectrum of the sum of two different disturbances equals the sum of the power spectra of the two different disturbances. From this, it follows that all other properties combine in the same way, and the pressure, velocity components, and energy flux of combined wave systems can be found immediately. If the sum of the two power spectra yields a power

*This section is also a proof of the statement made on page 260. The argument is given for two superimposed small spectra, but it would also follow for two adjacent spectra, (page 260 of Part I).

$$\overline{\overline{W.P.}}^{yt} = \int_{-H}^{\overline{0}^{yt}} W.P.\,dz = \lim_{\substack{\bar{y}\to\infty \\ \bar{T}\to\infty}} \int_{y_R}^{y_R+\bar{y}} \int_{t^*}^{t^*+\bar{T}} \left(\int_{-H}^{0} P(x_R,y_R,z,t)\cdot u(x_R,y_R,z,t)\,dz \right) dt\,dy$$

$$= \frac{\rho g^2}{4} \int_0^{\infty} \int_{-\frac{\pi}{2}}^{\frac{\pi}{2}} \left[1 + \frac{2H\mu^2 I(\mu,H)}{g \sinh\left(\frac{2\mu^2 I(\mu,H)H}{g}\right)} \right] \frac{[A_{2RH}(\mu,\theta_R)]}{\mu I(\mu,H)} \cos\theta\, d\theta_R d\mu \qquad (12.49)$$

Given straight parallel beach contours, waves like equation [7.31], and crests parallel to shore.

$$\overline{W.P.}^{t} = \frac{\rho g^2}{4} \int_0^{\infty} \left[1 + \frac{2H\mu^2 I(\mu,H)}{g \sinh\left(\frac{2\mu^2 I(\mu,H)H}{g}\right)} \right] \frac{(A_R(\mu))^2}{\mu I(\mu,H)} d\mu = \frac{\rho g^2}{4} \int_0^{\infty} \frac{(A(\mu))^2}{\mu} d\mu \qquad (12.50)$$

$$H/H_o = \sqrt{\frac{1}{2n} \frac{C_o}{C}} \qquad (12.51)$$

$$n = \frac{1}{2}\left[1 + \frac{4\pi d}{L \sinh\frac{4\pi d}{L}} \right] \qquad (12.52)$$

spectrum which does not satisfy the conditions imposed in Chapter 11, then the sea surface in the region of superposition will break up due to non-linear effects. However for swell arriving from a distance this effect is usually of no importance and thus most refraction problems are easily dealt with.

Consider equation (12.53). It states that given two power spectra, $[A_{2HI}(\mu,\theta)]^2$ and $[A_{2HII}(\mu,\theta)]^2$ for two different wave systems present at the same point and time of observation, then the total effect is obtained by adding them point for point and calling the sum $[A_{2H(I+II)}(\mu,\theta)]^2$. If equation (12.53) is true, then a similar equation holds for any number of power spectra, and the statements made in the paragraphs above are proved. All of the steps are valid for both deep water and the transition zone so that H can also be infinite in any of the equations which follow.

Now, $[A_{2HI}(\mu,\theta)]^2$ substituted into an equation like (9.47) would yield an expression for a sea surface which will be called η_I, and similarly $[A_{2HII}(\mu,\theta)]^2$ would yield η_{II}. Consider the power contributed to some one net element in the μ ,θ plane, upon passing to the limit inside the one net element, and consider that part of the total integral contributed by $\eta_{\Delta I}$ and $\eta_{\Delta II}$ which involves these power contributions. Let ΔE_I be the power contributed by $A_{2HI}(\mu,\theta)$ to $\eta_{\Delta I}$ and let ΔE_{II} be the power contributed by $E_{2HII}(\mu,\theta)$ to $\eta_{\Delta II}$ as defined by (12.54).

Then points chosen at random from $\eta_{\Delta I}$, either as a function of time at any fixed point or as points chosen from the whole x,y,t space, will be distributed according to equation (12.55). Points chosen at random from $\eta_{\Delta II}$ will be distributed according to equation

(12.56). From the derivations of the power integrals involved, there is no correlation between $\eta_{\Delta I}$ and $\eta_{\Delta II}$, and the two distributions are independent. These statements follow from the results of Chapter 7 and Chapter 10.

A theorem of statistics can now be used to prove equation (12.57). If two independent random variables are distributed according to the distributions given by equations (12.55) and (12.56), then the sum of the two independent random variables is distributed according to equation (12.57). For a proof of this theorem, see Cramer [1946] (page 212).

These equations hold for any net element anywhere in the μ,θ plane. They also hold for E_{Imax} and E_{IImax}. Thus the total power is the sum of the power of the two systems. Also the power in any net element remains in that net element. It follows immediately then that equation (12.58) holds and that the integrals which represent η_I and η_{II} combine according to equation (12.59) where the integration over θ may have to be from $-\pi$ to π. Then from the definition given in equation (12.53), the desired properties are proved.

If equation (12.59) is approximated by a finite net, it will be seen that the equation is not a true identity for the finite net. The equation is valid only in the limit, and to prove the equation for a finite net, it would be necessary to consider a sub net approaching infinitesimal areas inside of each net element.

No theoretical analysis or finite net is capable of resolving the spectrum of η_{I+II} into the spectrum of η_I and η_{II} if the power spectra overlap. However, if a swell power spectrum is added to a

Additivity of Power Spectra

$$[A_{2HI}(\mu,\theta)]^2 + [A_{2HII}(\mu,\theta)]^2 = [A_{2H(I+II)}(\mu,\theta)]^2 \tag{12.53}$$

Let ΔE_I and ΔE_{II} be the power in the same net element for $\eta_{\Delta I}$ and $\eta_{\Delta II}$ respectively (12.54)

$$p(\xi < \eta_{\Delta I} < \xi + d\xi) = \frac{1}{\sqrt{\pi \Delta E_I}} e^{-\xi^2/\Delta E_I} d\xi \tag{12.55}$$

$$p(\xi < \eta_{\Delta II} < \xi + d\xi) = \frac{1}{\sqrt{\pi \Delta E_{II}}} e^{-\xi^2/\Delta E_{II}} d\xi \tag{12.56}$$

$$p(\xi < \eta_{\Delta I} + \eta_{\Delta II} < \xi + d\xi) = \frac{1}{\sqrt{\pi(\Delta E_I + \Delta E_{II})}} e^{-\xi^2/(\Delta E_I + \Delta E_{II})} d\xi \tag{12.57}$$

$$\eta_{I+II} = \eta_I + \eta_{II} \tag{12.58}$$

$$\int_0^{\infty}\int_{-\pi}^{\pi} \cos\left[\frac{\mu^2}{g} I(\mu,H)[x\cos\theta + y\sin\theta] - \mu t + \psi(\mu,\theta)\right] \sqrt{[A_{2HI}(\mu,\theta)]^2 d\mu d\theta}$$

$$+\int_0^{\infty}\int_{-\pi}^{\pi} \cos\left[\frac{\mu^2}{g} I(\mu,H)[x\cos\theta + y\sin\theta] - \mu t + \psi(\mu,\theta)\right] \sqrt{[A_{2HII}(\mu,\theta)]^2 d\mu d\theta}$$

$$=\int_0^{\infty}\int_{-\pi}^{\pi} \cos\left[\frac{\mu^2}{g} I(\mu,H)[x\cos\theta + y\sin\theta] - \mu t + \psi(\mu,\theta)\right] \sqrt{[A_{2H(I+II)}(\mu,\theta)]^2 d\mu d\theta} \tag{12.59}$$

Plate LXIX

low local chop power spectrum, then the methods of analysis presented in Chapter 10 will separate the two spectra.

Some properties of the refraction of short crested Gaussian waves

Consider the refraction of the most elementary short crested wave system possible as given by equation (8.1) or by equation (8.4). Let the angle in deep water between the two elemental crests be given by, say, thirty degrees. Given the discrete spectral period, it is then possible to find the apparent length of the crests in the direction of the crests in deep water.

If the system is approaching an uncomplicated coastline without crossed orthogonals for that discrete spectral component and without caustics, then the closer to the shore the system is studied, the more the angle between the elemental crests is decreased because the crests are more nearly parallel to the shore. Thus nearer shore the apparent crests are longer than they are in deep water.

For any power spectrum with discrete spectral components such as the one treated in equation (8.5), the same thing occurs, and, in the limit, for the continuous power spectrum the same results are accounted for by $\Theta(\mu,\theta_R)$ and $\Gamma(\mu,\theta_R)$.

If in addition, the power spectrum varies over a wide range of μ, the low μ values are amplified in general more than the high values of μ by the effect of the factor, D, in wave refraction theory. Consequently, as a short crested sea surface approaches a coast in many cases, the crests become longer and more well defined, and the "significant" period of a wave record near the shore becomes longer than the "significant" period of a record taken at the same time in deep water. The refraction of a short crested sea surface by

the use of the "significant" height and period is therefore just as much in error as the analysis of a pressure record in terms of these values. For sea conditions, the results are meaningless.

"En echelon" waves can also be treated by these considerations. Suppose that a given filter from some storm has a narrow θ band width and a wide μ band width. Then the waves in deep water will have relatively long crests. Upon refraction, the long narrow spectrum becomes an arc, and evaluation of the finite net would then show the "en echelon" effect. The apparent crests would be shorter along the crests after refraction than before refraction.

Some aerial photographs

In this section two very fascinating aerial photographs and some enlargements of parts of these photographs will be discussed in detail. These photographs were furnished by Mr. Dean F. Bumpus of Woods Hole Oceanographic Institution. They are both very clear-cut examples of the refraction of a Gaussian short crested sea surface. They were taken along the coast of North Carolina at Oracoke and Swash Inlet by the Coast and Geodetic Survey on January 24, 1945. Figure 33 is an aerial photograph over Oracoke. Figure 34 is an aerial photograph over Swash Inlet. Figures 35, 36, and 37 are enlargements of parts of figures 33 and 34 for easily recognized areas.

Both photographs show some very interesting features. In the deeper water on the right, the longer crests are at about an angle of forty-five degrees to the coast line. The lengths of the apparent crests are quite short. Half way between the edge of the photo and the coast, the crests are more nearly parallel to the coast and

Figure 33. Aerial Photograph over Oracoke.

Figure 34. Aerial Photograph over Swash Inlet

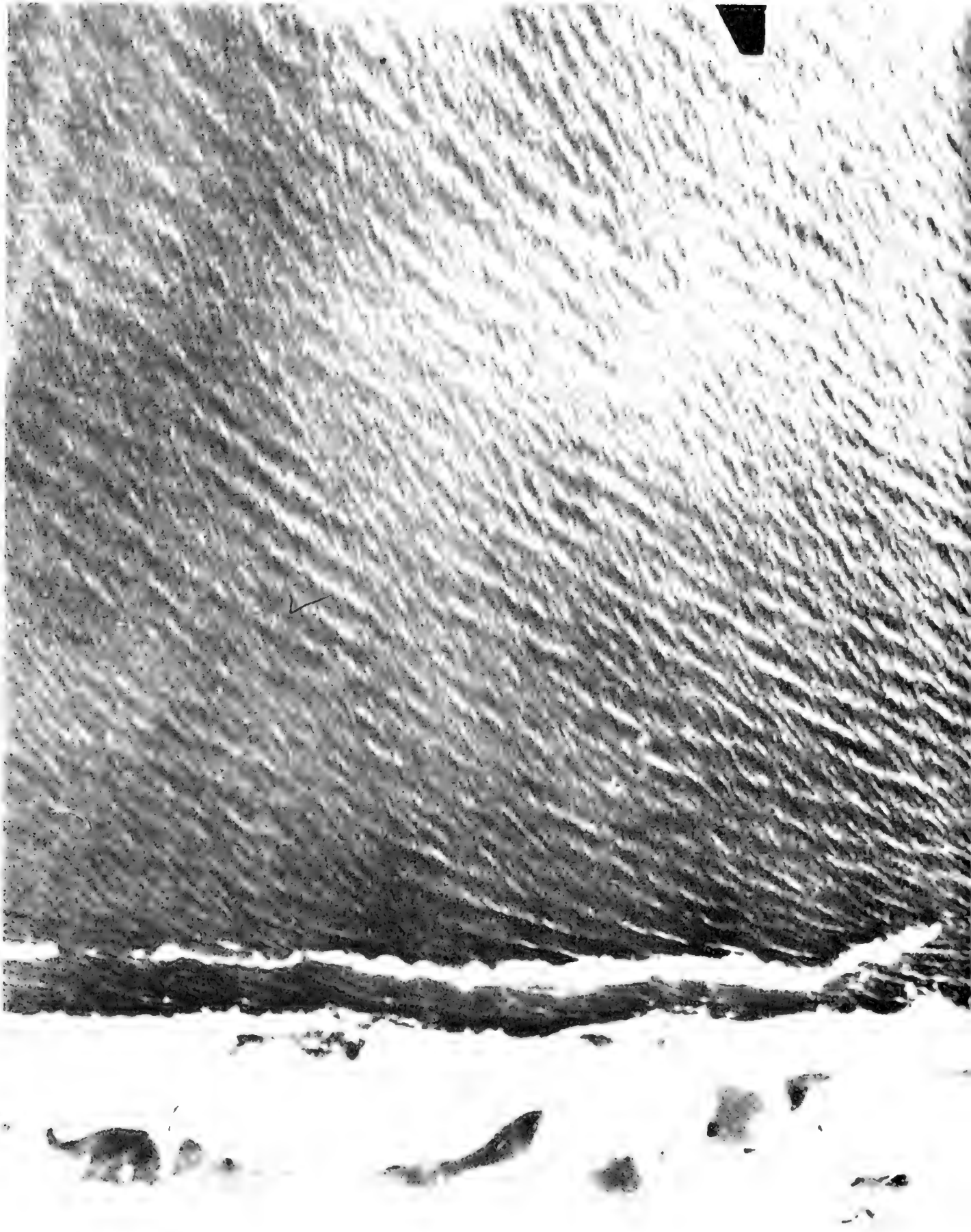

Figure 35 Enlargement over Oracoke

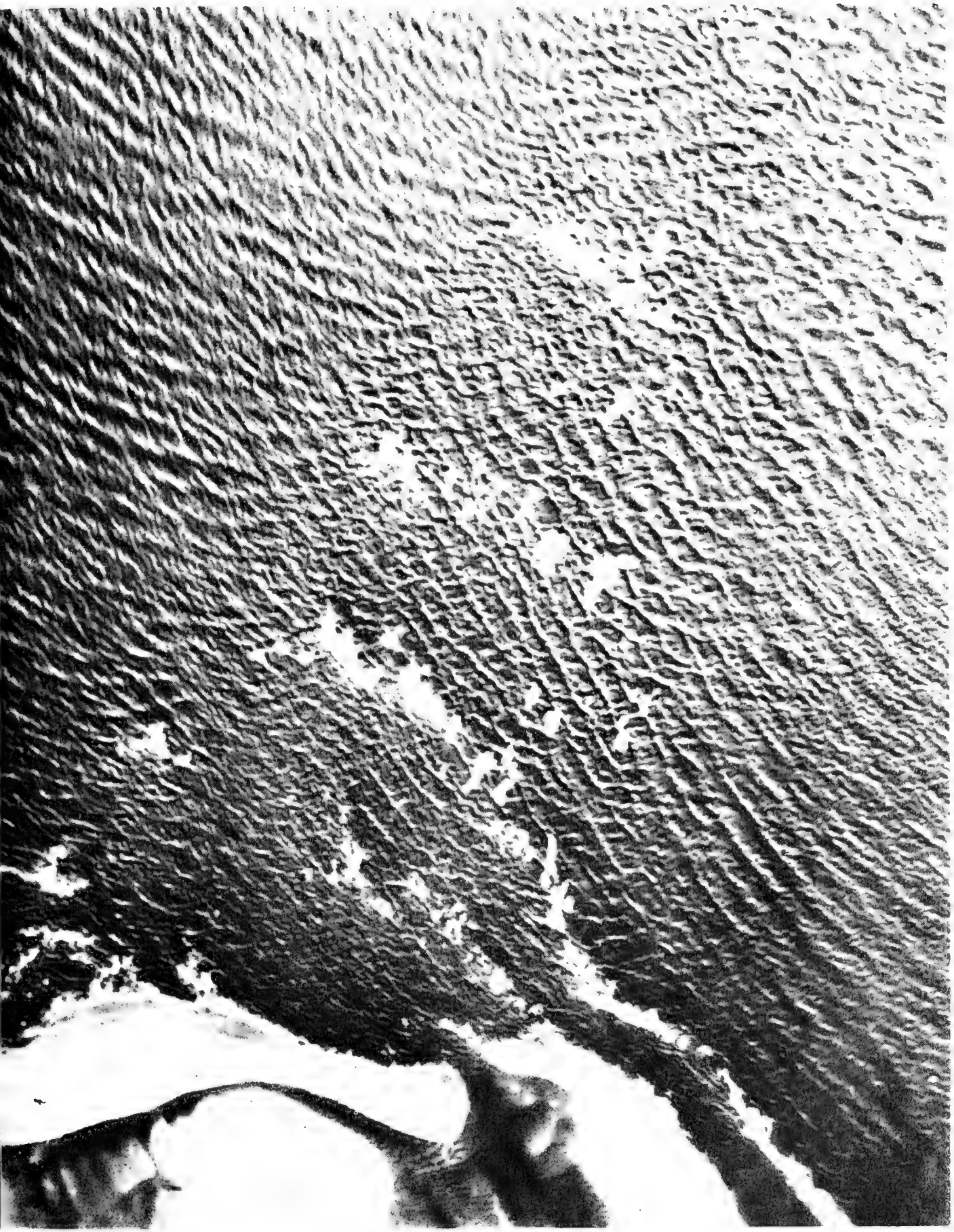

Figure 36. Enlargement over Oracoke.

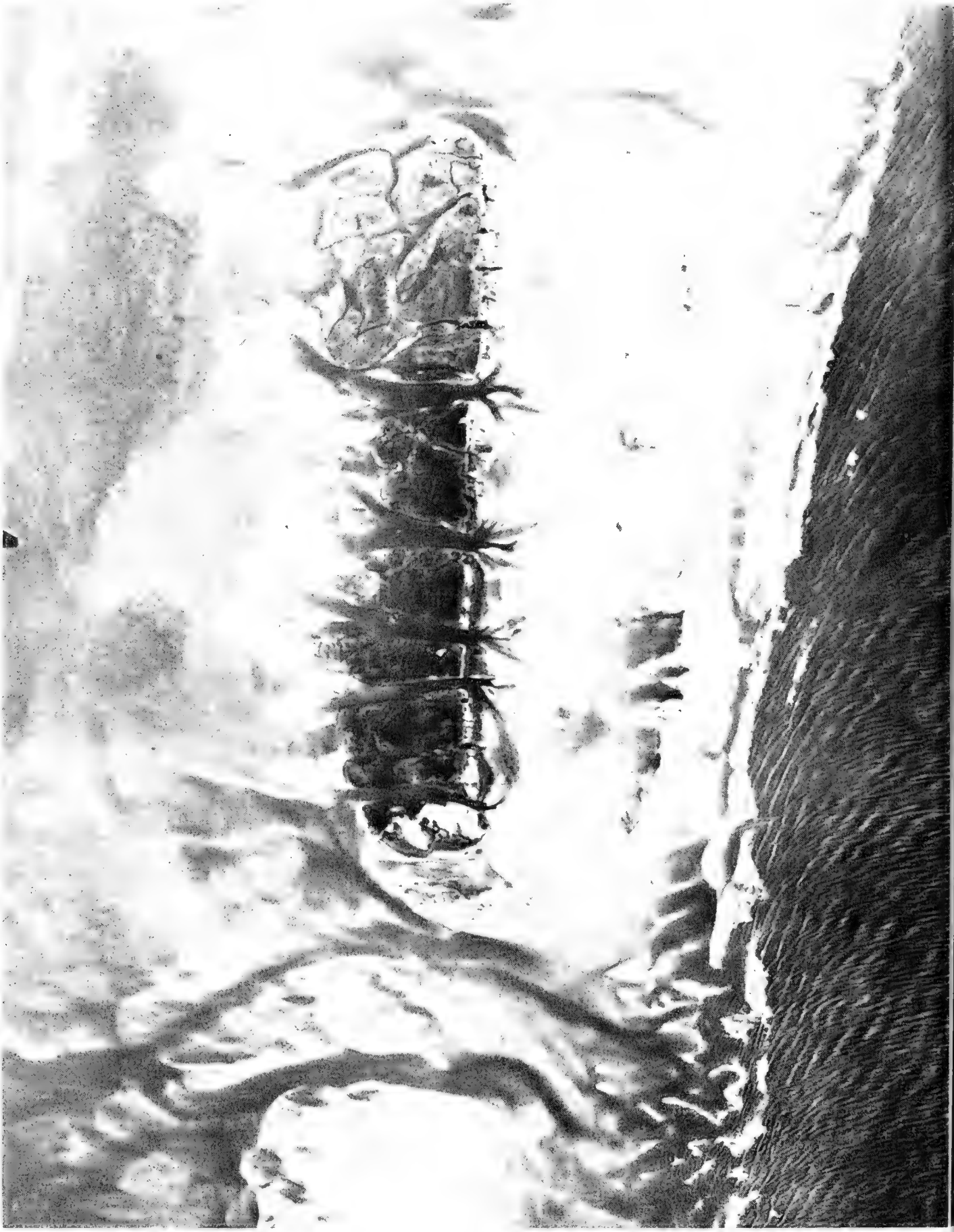

Figure 37. Enlargement over Swash Inlet.

the apparent crests are much longer. No individual crest can be followed very far by the eye before it becomes lost in an area of poor definition and low amplitudes.

A second interesting feature is the local chop which is superimposed on the longer apparent crests. At the far right, the crests are at about an eighty-five degree angle to the coast. Even near the coast, these short crested waves are only slightly affected by the bottom, and they have only turned a few degrees more parallel to the coast. The assumption of linearity, of course, assumes that neither system has an effect on the other which is not true for the higher order effects.

A third interesting feature is found by a careful study of the zone between the coast and a line about one-eighth of the distance to the outside edge of the photo and of the triangular zone at the base of the Oracoke photo. The crests in these zones do not have the same profile as the crests outside of the zones. The crests are higher and more peaked and the troughs are longer and shallower. Outside of the zones discussed above, the crests and troughs are equal in importance, and a graph (as a function of, say, distance along a dominant orthogonal) of the wave height would look very much like a wave record except that the apparent crests would be shorter near the coast. The outside edge of this zone and some curve probably off the picture define the transition zone studied in this chapter. Note that the local chop keeps on doing what it had been doing before even after the longer crests have been modified in profile (see figure 37).

The breaker zone

Between the curve defining the transition zone on the coastward side and the coast, non-linear effects are apparently dominant. From these photographs, Munk's Solitary Wave Theory [1949] may well be a first step in a study of this zone. This near shore zone is probably the location of the important beach erosion effects. In this paper, these effects as far as they can be treated by the methods used herein are covered in Plate LXX. In Plate LXX, only one point is emphasized. That point is that important non-linear effects cannot and must not be treated by the theories developed herein.

Summary of the past chapters

Methods and formulas which apply to storm generated ocean surface waves from the time they leave the edge of a storm at sea until they are just about to enter the zone where they break upon some coast have been presented in this chapter and in the past chapters. The procedures and techniques described apply realistically to waves as they are. They can discriminate between sea and swell. They can predict waves given data not currently available. They explain nearly all of the observed facts about ocean waves within the linearity approximation.

Two important problems have not been treated. They are the problem of the generation of waves and the problem of the breaking of waves in the breaker zone. Some general comments on wave generation will be made in a later chapter, but breaking waves will not be discussed.

The Solitary Wave Zone ?

The Breaker Zone ?

The Shallow Water Zone ?

NON-LINEAR

Plate LXX

Plan for the rest of the paper

The techniques and equations for the description of the sea surface have been presented in Chapter 5, and in Chapters 7 through 12. No more equations and derivations are needed as far as this paper is concerned, and thus there will be no more plates presented in the text.

In the next three chapters, these equations will be applied to practical data. An example of an accurate wave analysis will be given. The important numbers which can be obtained from such data will be computed. The character of wave records will be described in greater detail. A theoretical forecast will be carried out which will show the strange effects of refraction on the waves which reach the North Jersey coast. Wherever possible, published data and observations will be used to substantiate the results.

It should be pointed out that the derivations presented and the theoretical results obtained just scratch the surface of the results which can be obtained by continued investigation along the lines pursued herein. The problems of ship motion, radar reflectivity, the relationship between wave and wind spectra, capillary waves, circular storms, moving storms and very short range wave prediction are all still unsolved.

Chapter 13. EXAMPLES OF PRESSURE AND WAVE RECORD ANALYSES

Introduction

In this chapter, a detailed and highly informative analysis of a pressure record will be carried out according to the procedures devised by Tukey and Hamming [1949]. The pressure power spectrum will then be corrected for the effect of depth thus obtaining the power spectrum of the free surface. The 10% to 25% error of the significant height and period method will then be explained. Various features of the free surface will be deduced.

The analyses of wave record correlograms carried out by Tukey and Hamming will be discussed and interpreted in the light of some of the papers published by Seiwell [1949, 1950]. A refutation of the conclusion that wave records have one or more "discrete" periods (or cyclic components) will be given by showing that such components have not been proved to exist and that the available evidence correctly interpreted indicates the contrary.

The design criteria for wave analyzers as described by Tukey and Hamming will be applied to known wave analyzers and their performance will be interpreted in the light of these design criteria.

A detailed analysis of a pressure record*

The twenty-five minute pressure record which was sampled in Chapter 7 to see if it was Gaussian and which was taken on 18 December 1951 starting at 2258 EST can be analyzed and studied in great detail

* See also a paper to be published by Pierson and Marks [1952] in the A.G.U. Mr. Wilbur Marks has done all of the numerical work for this section and has written up the details of the procedures employed in the A.G.U. paper.

because it is long enough to yield reliable results. Before so doing, however, interesting results can be deduced just on the basis of the fact that the record is Gaussian.

The twenty-five minute record was recorded on ordinary chart paper (such as is shown in Figure 12) at a fairly rapid speed of 6 inches equal to one minute. The range of the record covers from extreme to extreme about seven or eight of the small chart divisions. The standard deviation of the record was found from one hundred points picked at random. An arbitrary zero was chosen as a line well below the record and the square root of the second moment about the computed mean of the sample as measured from this arbitrary mean was found. By some strange accident, the mean of the sample fell right on one of the scale lines within a few thousandths of a unit, and thus the estimated mean of the record falls, within the accuracy of the measurements, on one of the chart lines.

Now suppose that the mean and standard deviation of the sample which was taken are close to the true mean and standard deviation of the record. Then another sample of one hundred other points chosen at random would have nearly the same mean and standard deviation. In fact, an infinite number of different samples of points could be taken from the record and if the points were far enough apart, each sample would have essentially the same mean and standard deviation. More technically the means should be normally distributed with a mean near the true mean, etc. The only thing that could not be done would be to take a sample of one hundred points from, say, a portion of the record one second long such that the points were only one one hundredth of a second apart. In this case, since the

points are so strongly autocorrelated the distribution would not be Gaussian.

Also, all of the different samples could be combined into one big sample, and that sample would again have an approximately Gaussian distribution. And also if points were chosen, say, one one hundredth of a second apart throughout the total record length, then the 150,000 points so obtained would have an approximately Gaussian distribution.

Finally the distribution of every point on the whole record would be approximately Gaussian, and, since the record is continuous, this permits a computation as to how long a time out of the total twenty-five minutes the record will occupy a given range of pressure values. From equation (7.33) modified by a substitution of $P(t_1)$ for $\eta(t_1)$ and E_{PHmax} for E_{max}, it is possible to compute the probability that a point will exceed a certain value. If the probability that the record will exceed the value P_I is p(I) and if the probability that the record will exceed the value P_{II} is p(II), and if the value of P_I is greater than the value of P_{II}, then the probability that the value will lie between P_I and P_{II} is (p(II) - p(I)). Also (p(II) - p(I)) multiplied by the length of the record (25 min), then gives that fraction of the total time of the record that the pressure value will be between P_I and P_{II}.

For the record under study, one scale division was equal to 0.855 standard deviations. Therefore the probability that the record would lie between the scale line for the mean of the record and the scale line one unit above was equal to 0.3034, and theoretically for 7.58 minutes out of the total 25 minutes, the graph of the wave

record should have been between these two scale lines. As actually measured it was between the two scale lines for 8.03 minutes. This is a discrepancy of about 6% between the theoretical and observed values.

Table 18 shows the other values as computed from the theory and as checked by measurement. The greatest error in minutes is 0.45 minutes between the predicted and observed values. Thus the error in prediction is only about 2% of the total pressure record length. For the greater departures from the mean, the percentage errors are larger, but the whole table shows remarkable agreement between predicted and observed values. The last row, for example, predicts that the record will be more than three positive scale divisions from the mean for about eight seconds out of twenty-five minutes and that the record will be more than three negative scale divisions from the mean for another eight seconds. Actually the record never went below three scale divisions and it was above three scale divisions for ten seconds.

What has just been done should be reemphasized. Points were taken at random from a pressure record. The standard deviation of these points in terms of scale units on the paper was then computed. Then the total time that the record would occupy a certain range of values was computed on the basis of the fact that the record was Gaussian. The predicted and observed values were found to agree remarkably well out to 2.5 standard deviations of the distribution. Usually statisticians are well pleased if an observed distribution fits a normal curve two standard deviations away even crudely, and in this case the agreement is even good 2.5 standard deviations away.

Table 18. Predicted and observed total time during which pressure record occupies a portion of the graph of the 25 minute record

Chart scale units	Chart scale units Standard deviation in scale units	Probability	Predicted	Observed -	Observed +	Average $\frac{(+obs)+(-obs)}{2}$
0 to ±1.00	0 to ±.855	.3034	7.58	7.35	8.03	7.69
±1.00 to ±2.00	±.855 to ±1.71	.1529	3.83	3.78	3.82	3.80
±2.00 to ±3.00	±1.71 to ±2.56	.0382	0.931	1.12	0.64	0.88
±3.00 to ± ∞	±2.56 to ± ∞	.0055	0.138	0.00	0.17	0.085
		.5000	12.48	12.25	12.66	
			x 2		+12.25	
			24.96		24.91	

Note that the average values give very good agreement. They seem to remove the remaining non-linear effects in the pressure record explainable by a tendency toward a trochoidal form.

A very simple statistic therefore describes many of the features of the record. Were it actually a wave record, this statistic could have been forecasted by forecasting the power spectrum and integrating the power spectrum of the wave record over μ and θ to find E_{max}. Consequently, without even mentioning the significant height and period, important information can be obtained about the forecasted waves.

If the above record had been a wave record, it would be possible to predict, for example, that a given spark plug on a recorder like the one developed by the Beach Erosion Board (Caldwell [1948]) would be submerged for 4.90 minutes during the next twenty-five minutes, and the actual observed time would have been 4.63 minutes. If the waves were passing, say, an oil drilling rig in the Gulf of Mexico, (and if the rig could be located at a point compared to the dimensions of the waves), then the length of time the water would cover any given mark on the rig could be predicted. These considerations would not be valid for a free floating object like a life raft because it moves horizontally with the waves, but it is not too difficult to visualize extensions which would yield information on the motion of the raft above and below mean sea level also. A ship with a length comparable to the wave lengths associated with the spectral periods involved in the power spectrum would have a different up and down motion, but again the Gaussian character of the motion would have to be true and statements similar to the above could be made about the ship's motion.

The autocorrelation function in a detailed analysis of a pressure record

The autocorrelation function was not determined by the procedures given in Chapter 10 and equations (10.29) and (10.30). Such a computation is laborious, and instead the record was mechanically autocorrelated by the machine described by Seiwell [1950a]. Eighty lags of two seconds each were evaluated and the values were corrected so that they essentially correspond to the Q_p of equation (10.30) apart from a constant factor. Reduction of Q_o to unit value then yields the normalized autocorrelation function, and multiplication of each value by E_{PHmax} which is known from direct computation of the standard deviation of the Gaussian distribution would then yield the non-normalized autocorrelation function.

Since the record was taken in 30.5 feet of water, two second lags were used with the assurance that aliasing would be negligible. From considerations in Chapter 10, only about two per cent of the height of a 4 second elemental component would show up in the pressure record.

The autocorrelation function given at the top of figure 38 shows several interesting features. It dies out in a few oscillations to low values after about 18 lags (or after 36 seconds). Then it recombines to rise again to values near 0.15 after 26 lags (or after 52 seconds). After 56 lags, the autocorrelation function dies down to small values and from then on it never amounts to anything substantial again rarely assuming values near 0.10.

If there had been one pure sine wave component (or cyclic component) present in the record of an amplitude containing great enough

power to contribute an important part to the total power, then the autocorrelation function would not have died down completely and there would have been a cosine wave present out at the far end of the autocorrelation function.

If there had been several pure sinusoidal waves present in the record, it is possible that by accident they would be in phase cancellation at the end of the number of lags shown. Under these conditions more lags might show that the autocorrelation function would rise to more substantial amplitudes.

Thus it is proved that this record does not contain one pure sine wave of appreciable amplitude. No finite number of lags can prove the absence of several discrete sine waves (several can be 3, 5 or 50). A finite number of lags only makes it more and more unlikely that there are some given number of pure sine waves present. With more lags, one is more sure that a small number of discrete components are not present.

Although it is possible for there to be several pure sine components of appreciable amplitude in this record, the autocorrelation function seems to contradict the possibility of just a few, say one, two, or three. Also the fact that the record is Gaussian, seems to suggest that the record is of the form of equation (12.19) although again a few pure sine waves of low amplitude plus a superimposed Gaussian disturbance would yield an autocorrelation function quite similar to the one obtained, and the sampling procedures of Table 18 above might not detect any difference. The presence or absence of "cyclic" or purely periodic discrete components in wave records in general will be discussed in detail later in this chapter.

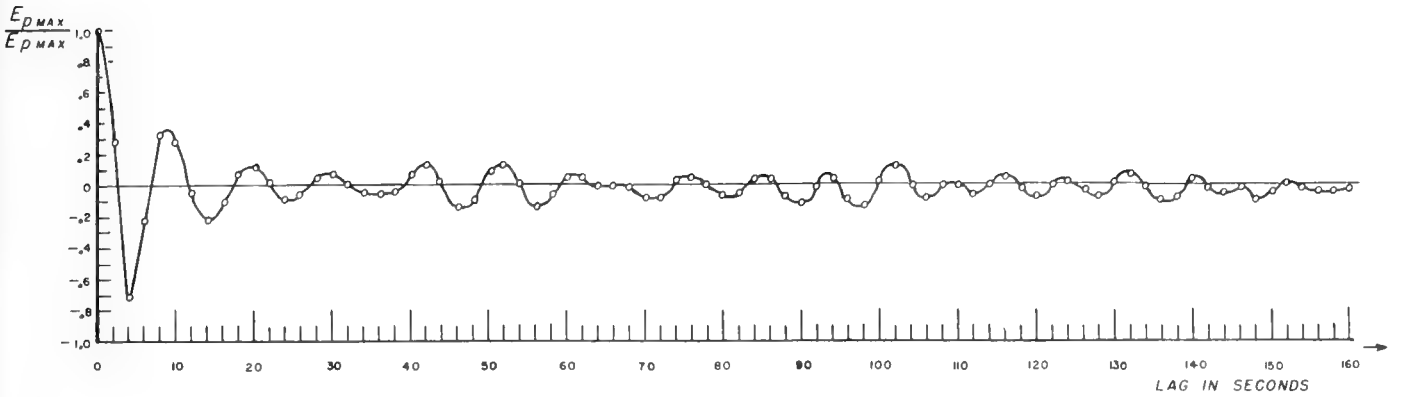

NON-NORMALIZED AUTO-CORRELATION FUNCTION
REDUCED TO UNIT AMPLITUDE BY DIVISION BY $E_{p\,MAX}$
FOR PRESSURE RECORD OF 10-18-21 FROM 2258 TO 2323 E.S.T.
AT A DEPTH OF 32.5 FEET M.S.L. OFF LONG BRANCH, N.J.

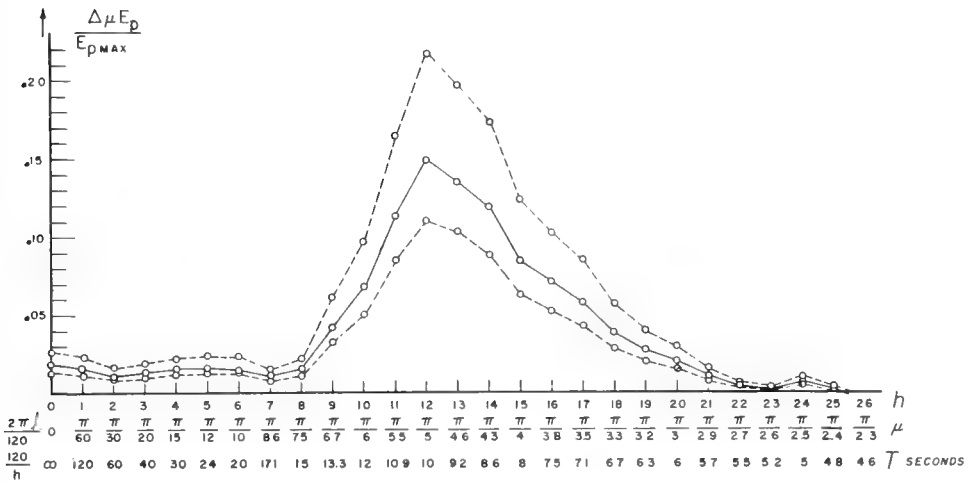

BEST ESTIMATE OF THE PRESSURE POWER SPECTRUM
OF ABOVE AUTO-CORRELATION FUNCTION IN TERMS OF
FRACTION OF TOTAL POWER PER UNIT BAND OF THE
μ AXIS. SUM OF VALUES AT $\mu = \frac{2\pi h}{120}$, $h = 0,1,2,\ldots 30$ IS EQUAL TO 1.018

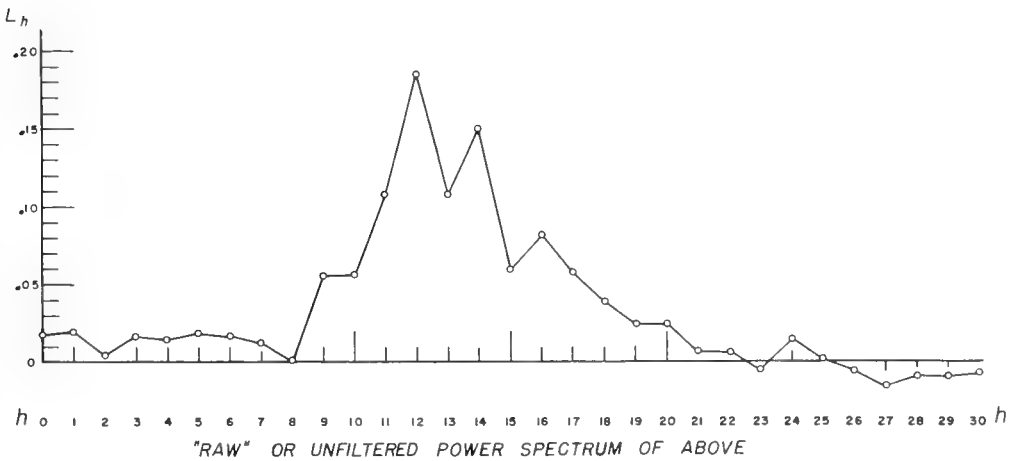

"RAW" OR UNFILTERED POWER SPECTRUM OF ABOVE

Fig 38. The Analysis of a Pressure Record

The "raw" pressure power spectrum

The next step in the analysis under discussion is to apply equation (10.31) to the normalized autocorrelation function given on the top of figure 38. The value of m was chosen to be equal to 30 in order to retain a sufficient number of degrees of freedom for each band. The use of the entire function would more than treble the labor involved and the results would be very unreliable (see Table 16 and equation (10.39)). The result of the computation is shown on the bottom of figure 38. The "raw" estimate is irregular, and were it to represent a power spectrum there might be reason to suspect that great difficulty would be encountered in attempting to forecast ocean waves.

The "filtered" pressure power spectrum

However, as has been shown, the "raw" estimates must be smoothed by equation (10.32) and upon smoothing the beautifully regular estimate is obtained which is shown in the center of figure 38. From Table 16 for 50 degrees of freedom, the true value in each band will be between 1.45 and 0.74 times the value indicated by the solid curve. These bounds are shown by the dashed lines on the figure. The sum of the values given on the solid curve is very nearly one, and this is both to be expected and to be considered a good check of the accuracy of the computations since the normalized autocorrelation function was employed. These results, upon the proper choice of scale, will yield the estimate of the true pressure power spectrum.

Quantitative interpretation of the filtered pressure power spectrum

So far for reasons of convenience, all of the computations have

employed the normalized autocorrelation function and in figure 38 the power under the spectrum is essentially one (a 2% error due to rounding seems to have occurred). The total power under the power spectrum is known from the results of Chapter 7, and it is now a simple and straightforward procedure to modify the ordinate scale of figure 38 in order to obtain the complete representation of the power spectrum given by the top part of figure 39. The scale on the left is in units of cm^2-sec and ranges from zero to slightly above 2000 units. Suppose that the peak is at 1700 cm^2 sec. Then the power from 2π 23/240 to 2π 25/240 (or from 10.43 to 9.60 seconds) is given by 1700 times $2\pi/120$ or by 88.8 cm^2. This is equivalent in power to a sinusoidal component 9.41 cm high.

Many interesting things can be deduced about the original wave record from the pressure power spectrum. Important amounts of power are contributed to the pressure record over the entire band, and all values of μ from $2\pi/15$ to $2\pi/6$ are important.

A finite net such as those described in Chapter 7 would thus require <u>at least</u> 12 sine components to <u>approximate</u> the record. All components would be of the same order of magnitude in amplitude. Even if no autocorrelative function were available, the power spectrum would show that a pure sine wave component with, say, 3/4 of the total power in the record is not present because the power spectrum would be markedly different from what it actually is.

There is reason to believe that "white noise" (Tukey and Hamming, [1949]) has been introduced into the data by the process of analysis since the original values could be read accurately to only about three significant figures. If so, then the small amount of power (about 10% of the total) indicated below $2\pi/15$ is not really present.

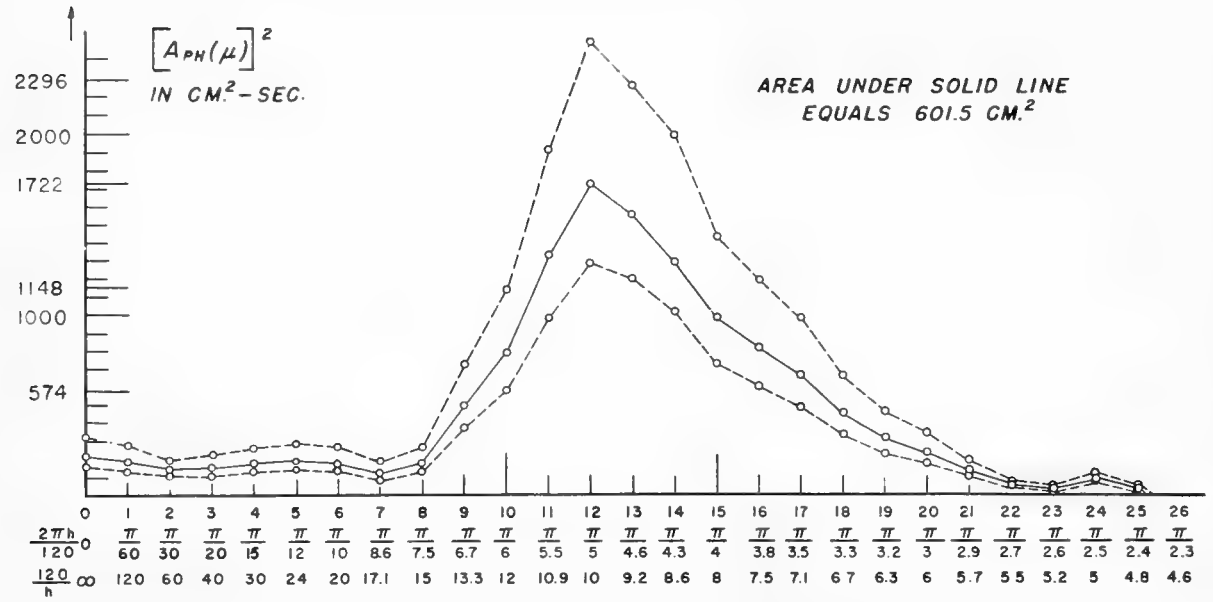

BEST ESTIMATE OF THE PRESSURE POWER SPECTRUM OF THE AUTOCORRELATION FUNCTION PLOTTED IN TERMS OF $[A_{PH}(\mu)]^2$ Vs. μ.
TRUE SPECTRUM LIES BETWEEN DASHED BOUNDRIES 90% OF THE TIME.

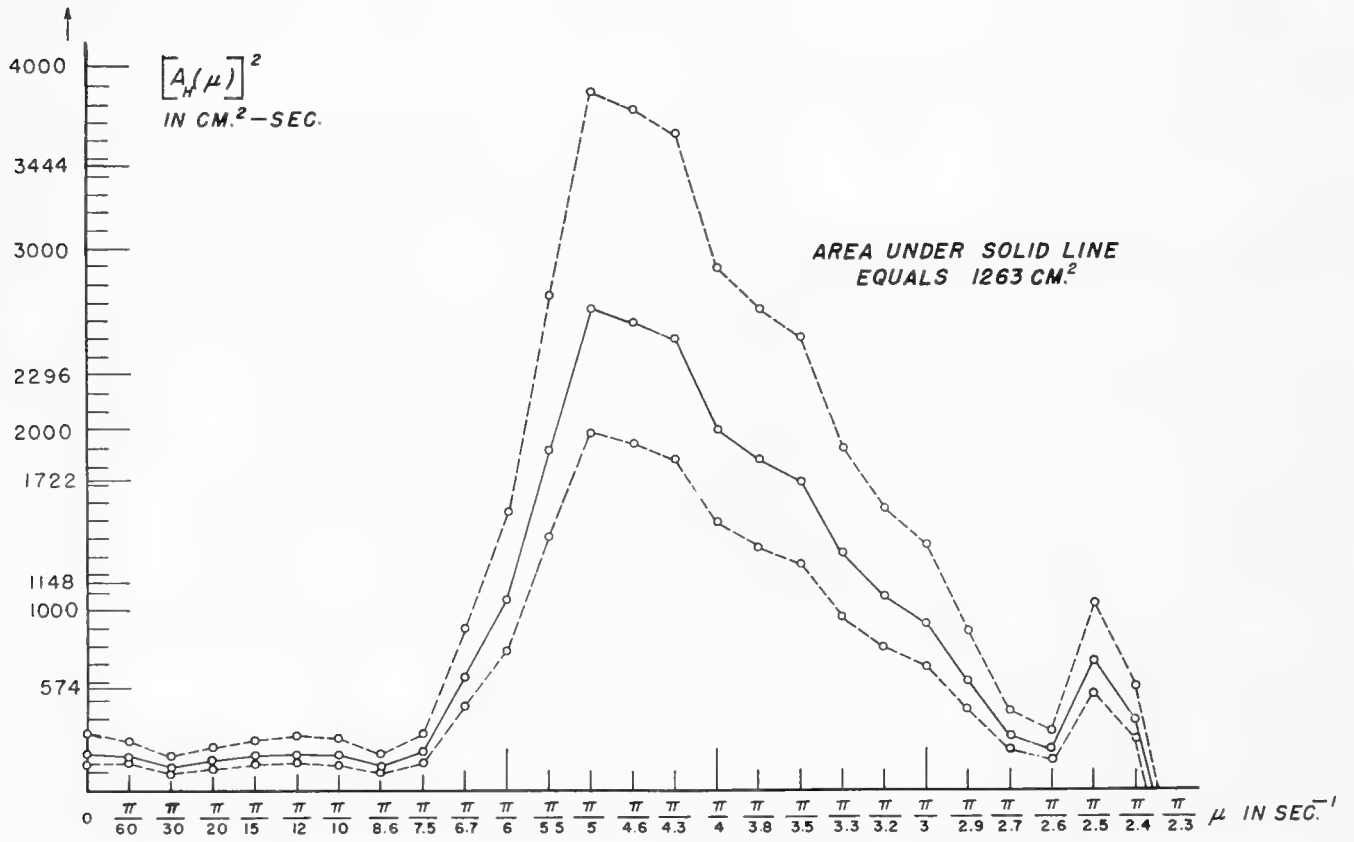

POWER SPECTRUM OF THE FREE SURFACE, $[A_H(\mu)]^2$

Fig 39. Quantitative Power Spectra of the Pressure Record and the Free Surface

The points determined by the circles represent the average value of $[A_{PH}(\mu)]^2$ over the band which straddles the point. The curve joining the points is simply an aid to the eye since any curve can be drawn over each band under study just as long as the area under it equals the value which has been determined. Thus the true power spectrum can be an extremely irregular function with very rapid (even if continuous) fluctuations. Even worse than that the power spectrum could have been of the form discussed in Chapter 10 and the same graph would have been obtained in figure 39.

To discover if really rapid fluctuations in the power spectrum are present, it would be necessary to increase m and the length of the record. Thus a 50 minute record and twice as many lags would give 60 bands of the μ axis instead of 30 with the same reliability. A 100 minute record with 120 lags would give four times as many values. Would the 120 values (instead of 30) thus determined follow the same general curve as shown by the solid line? The question cannot be answered until the work is done, (and it is not planned to do it), but it is very difficult to think of any physical mechanism which would cause the power spectrum to be irregular within any conceivable limits of resolution.

The above process of narrowing the band width and increasing the length of the record would also detect any purely sinusoidal component in the record. Thus with greater resolution, a discrete component would produce a sharp narrow spike rising out of the general function. The spike could be made as high as desired and as narrow as desired, and in the limit it would become infinitely high and infinitesimally wide such that the product of the height and the width

would be equal to the square of the amplitude of the discrete component.

Thus, to within the resolving power of the analysis which has been carried out, there is no proof of the presence of any discrete components, nor is there any proof that they are not present. A little thought shows that one can never prove either the presence or absence of very small power discrete components by taking one finite section of a time series since there is always the possibility that the function being studied is represented by a sum over a finite net such as in Chapter 7 with many more terms than could possibly be resolved by the choice of m and N in the numerical analysis.

The power spectrum of the free surface

The analysis of the pressure record given above has yielded the power spectrum of the pressure record. The time has now come to put back the high frequency waves (low period) filtered out by the effects of depth. The power spectrum of the free surface will be the result. The filtering process is not completely reversible because the waves with periods below four seconds have been irretrievably lost. Since the water is essentially infinitely deep for these low periods, a modified application of the results of Chapter 11 could estimate the amount of power left out completely.

It will be assumed that the pressure recorder responds to the actual pressure fluctuations at its indicated depth. This statement is equivalent to stating that purely sinusoidal pressure fluctuations at the depth of the instrument and of equal amplitude but different periods are recorded with the same amplitude.

The procedures are then straightforward and the results of

Chapter 12 apply. Each spectral band must be multiplied by a different correction factor as given by equation (12.21). The power spectrum on the bottom of figure 39 is then the power spectrum of the free surface. The true power in each band will lie between the dashed lines 90% of the time and the solid curve is the best estimate of the power spectrum.

Figure 40 is a comparison of the pressure power spectrum with the free surface power spectrum. It shows that the low period end of the power spectrum has to be amplified very much more than the high period end. The minor wiggle in the pressure spectrum at a period of 5 seconds may even be an important secondary peak in the free surface record. The free surface record will be more irregular and choppy then the pressure record. The spectra also show that the "significant" (or "characteristic") period of the free surface wave record will be lower than the "significant" (or "characteristic") period of the pressure record.

It is now possible to see where the 10% to 25% error described by Snodgrass [1951] comes from when the "significant" (or "characteristic") period is used along with the "significant" height to go from a pressure record to the waves at the free surface. The "significant" height is crudely proportional to the square root of E_{max} and the "significant" height of the pressure record is crudely proportional to the square root of E_{Pmax}. The "significant" period method of pressure record analysis multiplies $(E_{Pmax})^{1/2}$ by a constant amplification factor $[\cosh (\mu_1^2 H/g)\ I(\mu_1, H)]$, for a fixed μ_1 which depends on the choice of the "significant period. This choice varies from analyst to analyst on the same record.

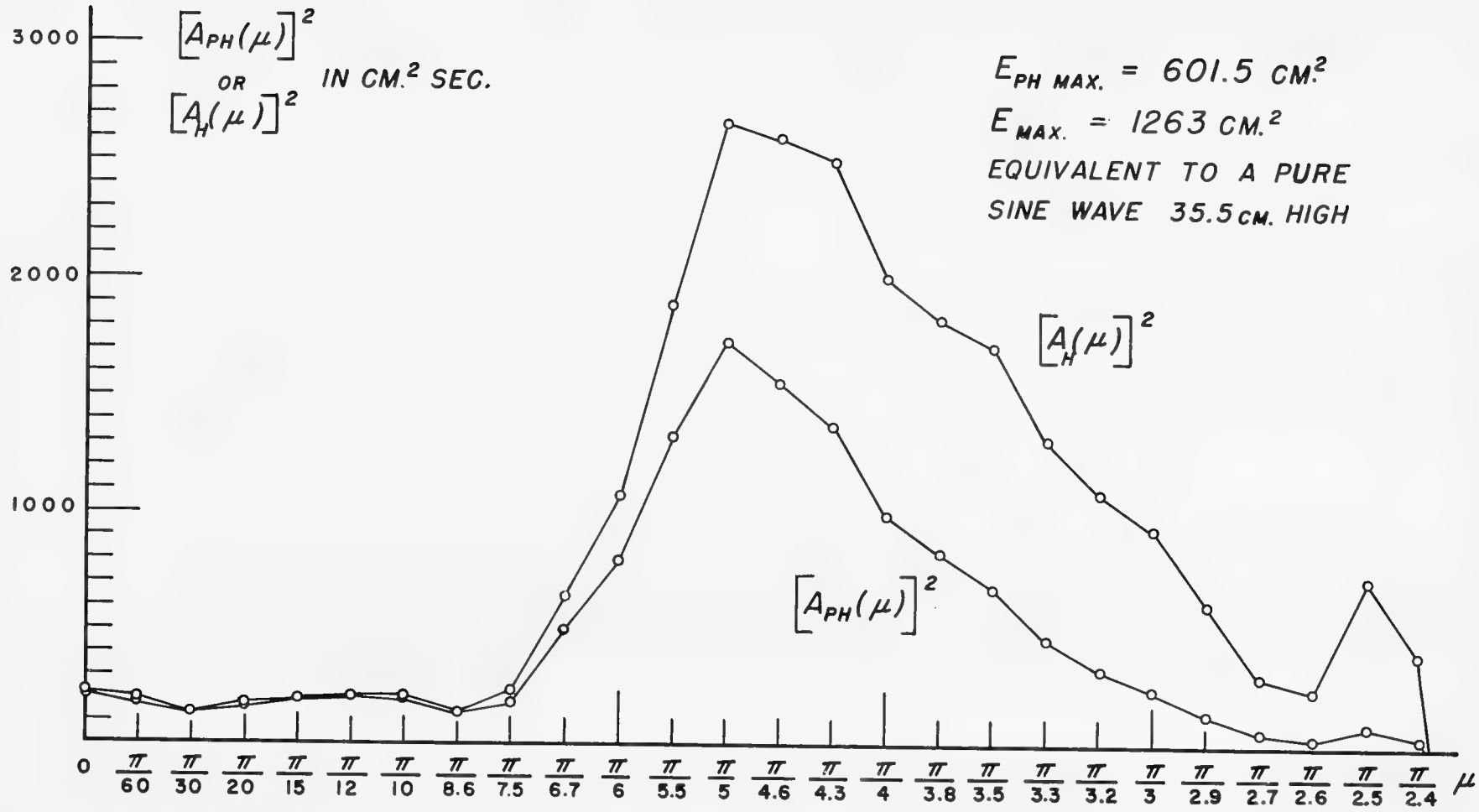

COMPARISON OF PRESSURE POWER SPECTRUM WITH THE FREE SURFACE POWER SPECTRUM. NOTE THE MUCH GREATER AMPLIFICATION OF THE LOW FREQUENCY COMPONENTS.

Fig. 40. Comparison of the Pressure Power Spectrum with the Free Surface Power Spectrum

Consider then a range of possible "significant" periods (depending upon the analyst) and the multiplication of the "significant" height of the pressure record by the possible amplification factors. Then the quantity

$$[(E_{max})/[\cosh(\frac{\mu_1^2 H}{g} I(\mu_1,H))]^2 E_{Pmax}]^{1/2}$$

is a ratio which represents roughly the value obtained by the correct method divided by the value obtained by the erroneous method. If the ratio were one then the error would not be apparent; if it is greater than one then the part after the decimal point represents the percentage error referred to by Snodgrass [1951]. Table 19 gives some of the ratios which can result from the assumption of various significant periods.

Thus for this depth, which is quite shallow compared to most depths at which pressure recorders have been installed, if the pressure record were given any "significant" period greater than 8.6 seconds, then there would be a considerable error in the computation of the "significant" height of the free surface. At greater depths and for differently shaped pressure power spectra the errors would be different and there is no hope of consistency in the old methods of analysis. Note that the power lost above 4.8 seconds would serve only to increase the error if it were included. Also note that the filtering nature of the pressure recording method always tends (given a widely variable power spectrum) to give too large a significant period to the free surface record and too small an amplification factor by the old methods.

Table 19. Ratio of correct significant height to value obtained by erroneous extrapolation of the pressure record upwards

Significant period (sec)	Amplification factor	Ratio
24.0	1.071	1.332
20.0	1.107	1.311
17.2	1.138	1.293
15.0	1.197	1.260
13.4	1.257	1.230
12.0	1.339	1.192
11.0	1.433	1.151
10.0	1.548	1.107
9.2	1.662	1.069
8.6	1.812	1.023
8.0	2.025	0.967
7.6	2.223	0.925
7.0	2.512	0.869
6.6	2.843	0.817
6.4	3.342	0.753

Significant height and period

The remarks so far in this paper have been in many cases directed against the concept of the "significant" (or characteristic) height and period method of wave analysis. There is really nothing wrong fundamentally with these concepts. The thing that is wrong is the way that the concepts have been misapplied.

The physical meaning of the average height of the one third highest waves, for example, can possibly be deduced from the power integrals and the autocorrelation function and the fact that the records are Gaussian. Such a number depends in a very complicated

way on the set of points in the record which determine the successive relative maxima and minima of the record. The probability distribution of this set of points may depend on the power spectrum in addition to the fact that the record as a whole is Gaussian. It is not too difficult to believe that the various ratios, 1/10 highest waves to the 1/3 highest waves, etc; such as summarized by Snodgrass [1951] are all consequences of the fact that the records are Gaussian. The trouble with these methods of analysis and of attempts to extend them such as those described by Putz [1950, 1951] is that the features of the wave record are obscured by concentrating attention too sharply on the waves. Paraphrasing an old saying: "such methods of analysis cannot see the wave record on account of the waves."

Similarly, the "characteristic" or "significant" period is a number determined from the time interval between successive relative maxima of the record if the relative maxima exceed a certain value. Given a high crest, the autocorrelation function says that the next crest is also likely to be high and that the next crest is most likely to occur at a time given by the first relative maximum after lag zero of the autocorrelation function. For a "swell" record the first maximum of the autocorrelation function has an amplitude which comes quite close to the original peak value and thus the "significant" period would have a useful meaning if the band width of the swell could be given. For a "sea" record the first relative maximum can be quite low, which means that the "significant" period is not a very useful number at all.

If the autocorrelation function in figure 38 is used to obtain the significant period of the pressure record studied at the start

of this chapter, then the value turns out to be about 9.2 seconds. Then from Table 19, the best estimate of the percentage error which would result from an incorrect upward extrapolation of the pressure record to the free surface is 6.9 per cent.

Seiwell's results

Publications by Seiwell [1949, 1950] and Seiwell and Wadsworth [1949] have claimed that a purely cyclic (or sinusoidal) component is present in wave records. Later the original interpretation was modified to include the presence of two or three cyclic components. The autocorrelation method is quite laborious, and the earlier conclusions were based on one second lags for the first complete "oscillation" of the autocorrelation function followed by skipping some arbitrary number of lags and then finding another "cycle." For example, if the autocorrelation record shown in figure 38 were given for only the first 10 seconds followed by no data from 12 seconds to 40 seconds and then by another cycle from 42 seconds to 52 seconds it might be very easy to conclude that one "cyclic" component was present. This conclusion is of course shown to be incorrect by the rest of the data. Once one cyclic component is found, then a little more detail in the autocorrelation leads to the hypothesis that several "cyclic" components are present.

Tukey's analysis of Seiwell's results

Tukey and Hamming [1949] have analyzed Seiwell's data, and although the autocorrelation function employed was normalized in a way which makes the values somewhat different from the correct procedure given in equation (10.30), the results are of interest here. The following paragraphs are quoted from Tukey and Hamming and figure

41 is a copy of the figure referred to in the quotation.

"The next two examples, provided through the kindness of Dr. H. R. Seiwell of the Woods Hole Oceanographic Institution, are based on pressure recordings taken off Cuttyhunk Island, Massachusetts in 1946. They represent the pressure at a depth of 75 feet and reflect wave heights. The basic data are:

Station	53-W	53-X
Date	15 Sept. 46	15 Sept. 46
Time	0500 hours plus 270 to 600 seconds	0650 hours plus 325 to 636 seconds
Serial correlations for lags of	0(1) 20 seconds	0(1) 16 seconds
Length of run	331 seconds	301 seconds

This type of data has been subjected to a few-constant fitting procedure based in part on quadratic autoregressive residuals as reported by Seiwell and Wadsworth --- and by Seiwell ---.

"In this case also, the serial correlations have been analyzed as if they were serial products.....The L_h* values obtained by a simple equating method, show substantial negative values. Since true negative values are impossible this makes such equating methods entirely useless on such data. The "U_h*" values, on the other hand, show a very reasonable behavior and, in particular are never negative by more than 0.004, which presumably results from accumulated errors and the use of r_p instead of Q_p.

"The upper frequency limit is 0.5 cycles/second for each record, since there is 1 sample/second. Thus for record 53-W we have a power density estimate every 0.025 cycles and for record 53-X every 0.03125 cycles. The results are plotted in [the] figure ..... We see that the general character of the results is the same, namely an unresolved peak near 0.075 cycle/second and essentially no energy beyond 0.15 cycle/second. The peak frequency may have increased in record 53-X as compared with 53-W.

"In order to study the nature of the peak near 0.075 cycles/second, it would be natural to repeat the analysis so that the upper frequency limit would be at, say 0.125 cycles/sec, which would be obtained by analyzing the record at 4 second intervals and using lags of 0, 4, 8, ..., 80 seconds. Unfortunately this would lead to widely fluctuating results since there would then be only 82 points in the longer record, and there would be only

$$\frac{82 - \frac{1}{4}(20)}{20/2} = 7.7$$

degrees of freedom for each U_h^* if m = 20 were again used. Thus any attempt to put the peak under too powerful a microscope is doomed to failure unless a longer stretch of observation is available. The length of the record, the spacing of the observations, and the lags used are ideally suited to show that there is essentially no power above 0.12 to 0.15 cycles/second (at periods less than 8.3 to 6.6 seconds), but is not well suited to the detailed investigation of the structure of the peak. The 53-X record has been analyzed by Seiwell and Wadsworth in terms of a combination of

(1) a single frequency, and

(2) an auto regressive scheme as proposed by Kendall....

The latter scheme would involve a finite amount of power in the region 0.12 to 0.50 cycle/second now seen to contain at most a negligible amount. Almost any analysis containing simple auto-regressive components will similarly fail to fit the observed facts."

The above analysis shows that the one second lags chosen and the number of lags made were quite inadequate to describe the power spectrum. At depths of the order of 78 feet, faith in hydrodynamic theory would tell us that all periods less than about 6 second would not be recorded by the pressure recorder and the spectra shown surely confirm this fact since essentially 2/3 of the values obtained are zero. Note that for a lag of three seconds and for the same amount of work on a record three times as long, considerable valuable information would have been obtained.

Noise versus signal

The problem of proving that a wave record contains one or several pure sine waves is analagous to a problem treated originally by Wiener [1949] in his famous book on communication theory. Consider an A.M. radio receiver a great distance from the transmitter. Let the detected signal, say, one of the notes in the chimes of

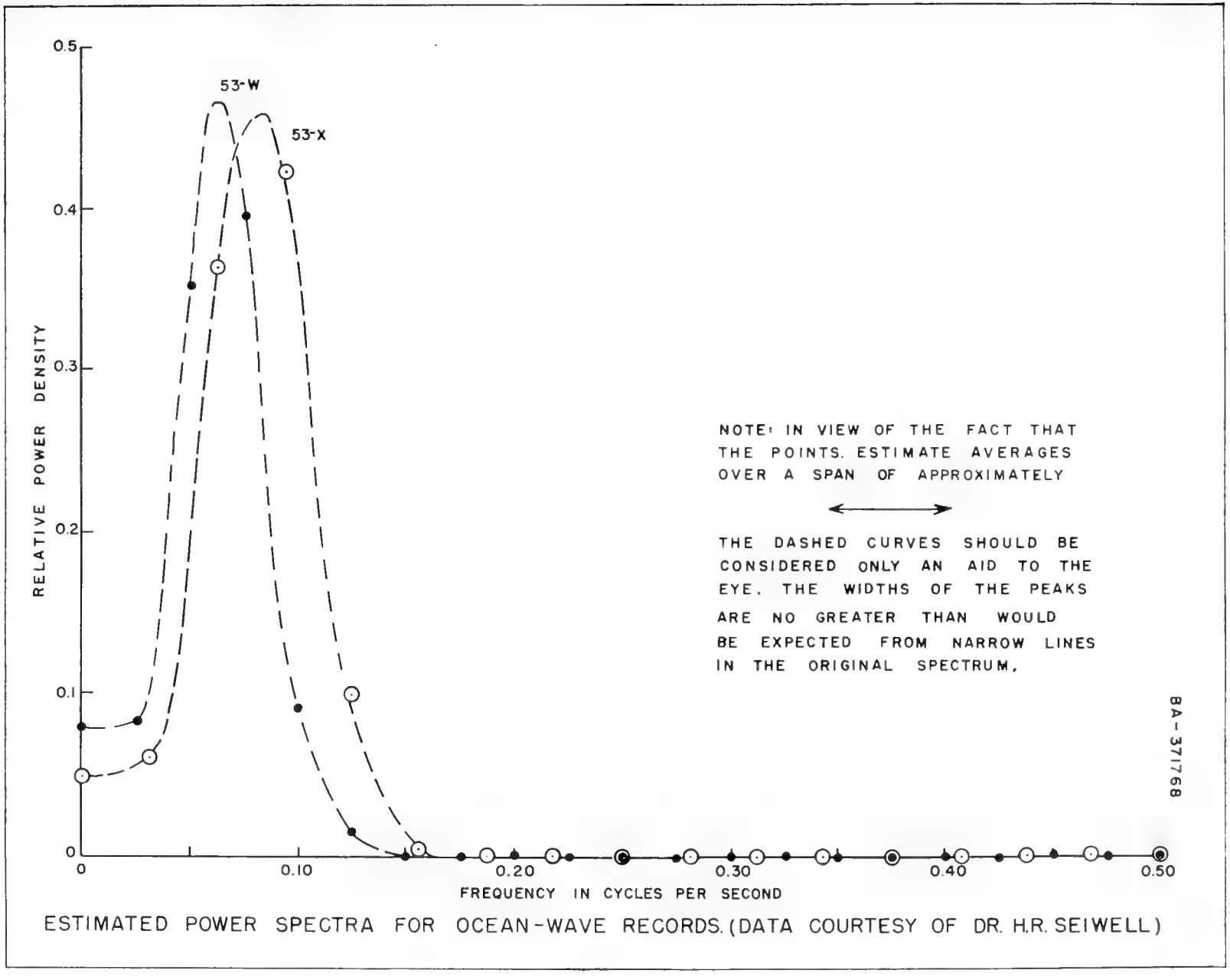

Figure 41. Power spectra computed from Seiwell's data (after Tukey and Hamming).

N.B.C., be so weak that it is drowned out audibly by static and tube noise. Also suppose that a long record of the voltage graphed as a function of time is available. The noise can be described by an integral similar to, say, equation (7.1). The chime would be the fundamental and harmonics of a pure sine wave. An autocorrelation of the record would cancel out the noise, and eventually the oscillation due to the sine waves would be all that is left. The discrete components correspond to jumps in the cumulative power density such as in the first examples in Chapter 7, and the noise yields a continuous increase between the jumps.

If the signal is very weak, many autocorrelations must be made and the weak oscillation cannot be detected until the autocorrelation of the noise has gone nearly to zero. If the signal is strong, not so many lags must be taken in order that it become visible as an oscillation in the autocorrelation function.

The cumulative power distribution functions for the case with cyclic components

Figure 42 shows two cumulative power distribution functions which illustrate the problems connected with the analysis of wave records. The first contains an easily recognizable cyclic component. The second contains many small cyclic components.

The upper one shows a discrete jump in $E(\mu)$ at $2\pi/T_1$. Let $\psi(\mu)$ at $\mu = 2\pi/T_1$ be $\pi/4$. The jump has about half of the power of the total record. Given this form for $E(\mu)$, then equation (7.1) would consist in part of a limiting form like equation (7.7) plus a pure sine wave of finite amplitude (equal to the square root of the jump in the record). With such a pure sine wave present, the distri-

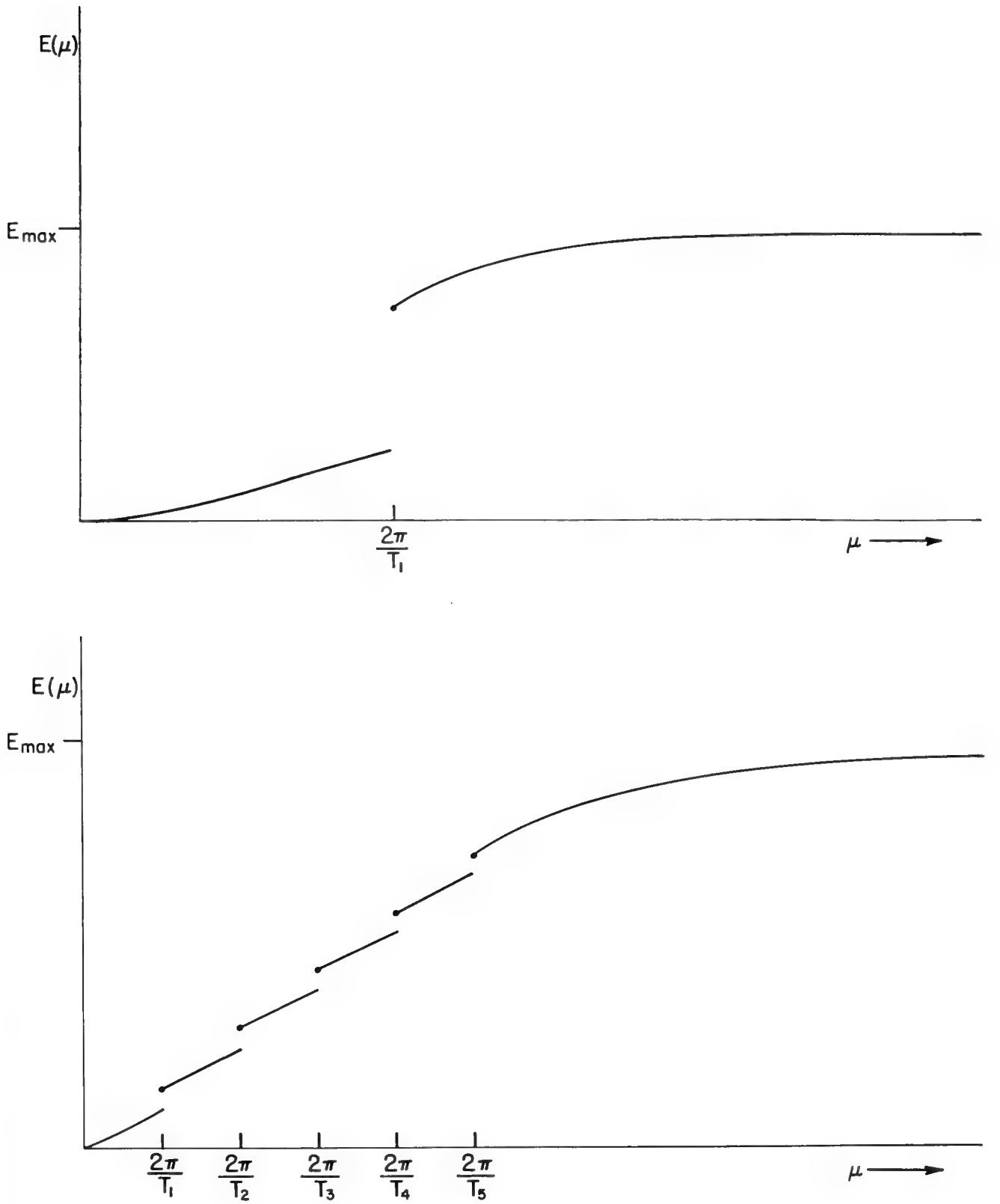

Figure 42. Some Cumulative Power Density Functions for time series with "cyclic" components present.

bution would be recognizably non-Gaussian. After a sufficient number of lags, the autocorrelation function would settle down to the form of a pure cosine wave with an amplitude equal to one half of the original power. The autocorrelation function could not possibly become small like the one shown in figure 38.

The lower cumulative power distribution function shows five small but still discrete jumps in $E(\mu)$. Again there would be a term of the form of equation (7.7), but now in addition there would be five pure sine waves present at $2\pi/T_1$, $2\pi/T_2$, $2\pi/T_3$, $2\pi/T_4$ and $2\pi/T_5$. (Let the phases be fixed by defining $\psi(\mu)$ at these points.) It would be quite difficult to detect these five pure sine waves by autocorrelating the record. However after enough lags, they would be all that remains of the record. If the record were truly stationary, in fact, the discrete components would still show up upon correlation of a record, say, 30 minutes long, with another record, say 30 minutes long, taken several hours later.

Final conclusions of the autocorrelation function

Thus by analogy to the above comments, the autocorrelation function of the record studied in figure 38 proves that there is not one pure sine wave present with an amplitude squared equal to 25% to 50 % (or greater) of the total average square of the record. It is not proved that there is no pure sine wave present with, say, an amplitude squared equal to 1% or .1% of the total average square of the record.

In the derivation of the theory of previous chapters, it has been assumed that wave records are essentially pure noise. The most powerful argument in favor of this assumption lies in computed power

spectra which show appreciable power in bands throughout the entire analysis. A second powerful argument lies in the spectra obtained by Barber and Ursell [1948] and Deacon [1949] which show a gradual essentially continuous shift as the power spectrum of a swell follows the theories derived herein. One is forced to conclude that discrete sine waves of appreciable amplitude have not been proved to be present in wave records, and that the best interpretation of a wave record is that it is just colored noise.

The flux of energy toward the shore

The free surface power spectrum given in figure 39 is a function of μ alone and nothing can be said about the short crestedness of the free surface. All power in the power spectrum for periods less than four seconds has been lost due to the filtering effect. Extrapolation of the high end of the spectrum suggests that the power lost above μ equal to $2\pi/4$ is not too great.

If it is assumed that most of the wave energy flux is in one direction and if this direction is assumed to be very nearly directly toward the shore since the winds were almost directly on shore, then the flux of energy toward the shore can be computed from equation (12.50).

The top part of figure 43 is a graph of the integrand of the integral given in equation (12.50) for the particular power spectrum under study with $\rho g^2/4$ absorbed in the scale on the left. For the depth under consideration (30.5 feet), values of μ near $2\pi/4$ seconds yield essentially the form $(\rho g/2)\cdot(A(\mu))^2\cdot(g/2\mu)$ which means that the energy flows forward with the group velocity of "deep" water waves, $(g/2\mu)$. For low values of μ, the energy is essentially moving

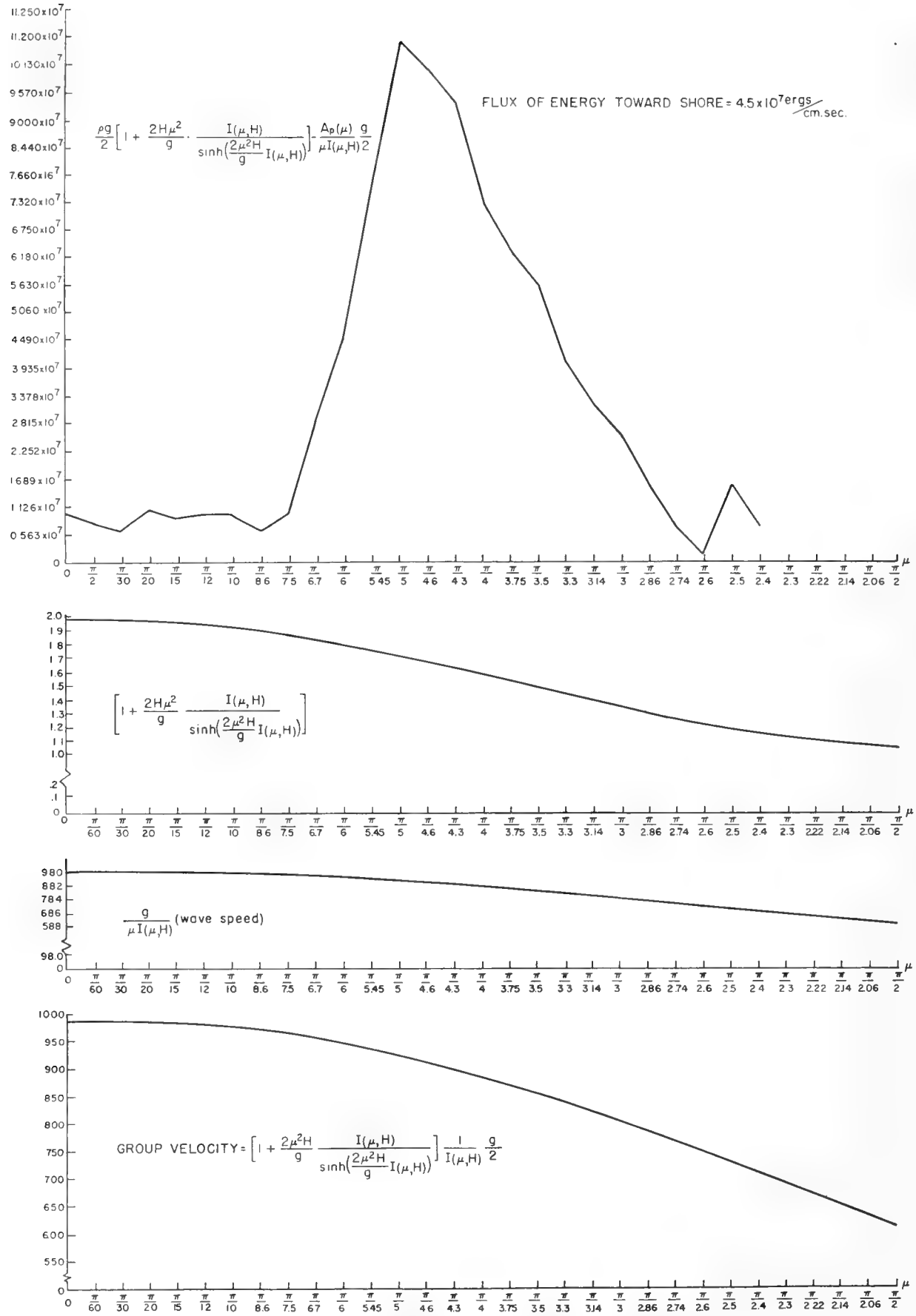

Figure 43. Graphs of the functions needed in the computation of the energy flux toward shore, and the integrand of equation (12.50) in the power spectrum given on figure 39.

forward with the speed, $(gH)^{1/2}$, i.e. the group velocity of shallow water waves.

The various terms involved in the computation of the top part of figure 43 are shown below the graph of the integrand of (12.50) for the case under study. The term in the square bracket, namely,

$$1 + \frac{2H\mu^2 I(\mu, H)}{g \sinh[\frac{2\mu^2 I(\mu, H) \cdot H}{g}]}$$

is graphed first. It ranges from the value of two to the value of one and is equal to two at μ equal to zero and asymptotically equal to one as μ approaches infinity. For practical purposes, it is equal to one at μ equal to $2\pi/4$. With a one half from out in front of the integral the graph is simply the classical expression, (12.52), graphed as a function of μ, i.e., $(2\pi/T)$, over the range of interest.

The other term, namely $g/\mu\ I(\mu, H)$, is the wave crest speed (a g is needed from out in front of the integral). At μ equal to zero, it equals $\sqrt{gH}$ and for large μ it approaches zero values (since capillarity is neglected). The value at μ equal to zero is 985 cm/sec since the depth is 991 cm.*

The bottom graph is the group velocity of the various spectral components. It equals 985 cm/sec for low values of μ and falls to half this value at $2\pi/5.4$. This graph times the energy in the wave record per band of the μ axis given by $(\rho g/2)[A_H(\mu)]^2 \Delta\mu$ then gives the flux of energy toward shore.

Finally, a numerical integration of the top of figure 43 yields the result that the energy flux toward the shore is equal to 4.58×10^7 ergs/sec per centimeter of length along the wave crest.

* The mean low water value was corrected to mean sea level, and a possible two foot tidal amplitude was neglected.

This is equivalent to 4.58 watts/cm, or along one kilometer offshore there are 458 kw of wave power flowing toward the shore in the vicinity of the point of observation. This amount of power is rather puny compared to values which can result from the action of high waves, but at least it is an accurate theoretical value based upon a sound analysis of the original pressure record.

Table 20 shows the numbers which are appropriate to the complete determination of the energy flux toward the shore as has been given above for the example being studied in detail. The first column is the number, h. The second column is the spectral frequency. The third column shows the values of the pressure spectrum in reduced units as it is shown in the center of figure 38. The fourth column shows the amplification factors for the pressure power spectrum. The fifth column shows numbers related to the group velocity. The product of the last three numbers across each row would yield a value for each spectral frequency and the sum of all of the values for each spectral frequency would be a number which, apart from a constant, would yield the energy flux toward shore.

The power per unit band in the pressure power spectrum varies over a factor of fifty from the greatest to the least. The amplification factor varies over a factor of ten and the group velocity factor varies from 2.01 to 0.85. Some of the values in the function to be integrated, which result from the product of these numbers, are thirty-eight times greater than other values. In the significant height and period method, one value for the significant height of the pressure record and one value for the significant period would result in an extremely inaccurate estimate of the energy flux toward shore.

Table 20. Numbers relevant to the computation of the flux of energy toward the shore

h	μ	Normalized pressure power spectrum	Amplification factor	Group velocity factor
0	0	.0178	1.00	2.01
1	$2\pi/120.0$	.0166	1.004	2.00
2	$2\pi/60.0$	.0119	1.008	1.99
3	$2\pi/40.0$	.0141	1.026	1.98
4	$2\pi/30.0$	.0161	1.049	1.97
5	$2\pi/24.0$	.0171	1.071	1.95
6	$2\pi/20.0$	.0163	1.107	1.928
7	$2\pi/17.2$	.0109	1.138	1.915
8	$2\pi/15.0$	.0161	1.197	1.875
9	$2\pi/13.4$	.0433	1.257	1.805
10	$2\pi/12.0$	.0685	1.339	1.745
11	$2\pi/11.0$	.1146	1.433	1.686
12	$2\pi/10.0$	.1501	1.548	1.630
13	$2\pi/9.2$	.1357	1.662	1.580
14	$2\pi/8.6$	.1199	1.812	1.524
15	$2\pi/8.0$	.0861	2.025	1.493
16	$2\pi/7.6$	.0718	2.223	1.408
17	$2\pi/7.0$	.0593	2.512	1.340
18	$2\pi/6.6$	.0400	2.843	1.272
19	$2\pi/6.4$	.0282	3.342	1.217
20	$2\pi/6.0$	.0214	3.787	1.149
21	$2\pi/5.8$	.0119	4.435	1.078
22	$2\pi/5.4$	.0048	5.480	1.012
23	$2\pi/5.2$	.0029	6.807	0.950
24	$2\pi/5.0$	.0075	8.225	0.918
25	$2\pi/4.8$	.0033	10.336	0.854
~	$2\pi/4.6$	~ 0	~	~

The number which finally resulted in the above computations is an important number for beach erosion problems. The result is valuable, but it is still a long way from the data which are actually needed. The wave direction is unknown, and the form of the breakers and the angle they make with the coast upon breaking cannot be determined from one pressure recorder and from the theories presented herein.

What percentage of the wave power moves sand at the beach, what percentage might have been surf beat actually flowing outward, what percentage is dissipated by friction when the waves finally break, and what percentage goes into the kinetic energy of a littoral current (if the waves are at a slight angle to the beach) are all questions for future theoretical investigation.

Wave record analyzers

Wave record spectrum analyzers have been reported in the literature by Barber and Ursell [1948] and Klebba [1946]. Wave record autocorrelators have been described by Seiwell [1950a] and Rudnick [1951]. The spectrum analyzers yield some function which is supposed to be some sort of spectrum of the record. They have no scale for the amplitude of the spectrum, and they have not been adequately calibrated.* Until the work of Wiener [1949] and Tukey and Hamming [1949] there was no way to interpret such analyses and there was considerable confusion on how the machines were to be constructed and on the design of the electronic circuits needed.

---

*As far as is known as of the date of this paper.

Compare the irregularity of these results and the lack of quantitative values with the numerical analysis which has just been presented. The spectrum was quite regular and the results were precise in a statistical sense. The accuracy could have been increased by taking a longer record and the results would be precisely defined.

A record of a given length, with a fixed degree of resolution, has a certain inherent statistical inaccuracy, due to the size of the sample and the band width of the analysis, which cannot be reduced; and Tukey and Hamming have described this inaccuracy and given the precise procedures for stating the results in a statistical sense.

The wave analyzers mentioned above have the same inherent errors (except possibly aliasing) as the results of the numerical methods plus others due to design characteristics. The analyzers can be redesigned so as to approximate the numerical method of analysis employed above, and, moreover, they can be calibrated against a numerical analysis in order to check their response.

The need for wave record analyzers

The numerical wave record spectrum analysis presented above required many months of work and effort. It would be impossible to analyze an adequate supply of wave records by the same slow computing techniques. One nice thing about the overall problem of forecasting ocean waves is that huge quantities of these records can be made available and much larger quantities will be becoming available from deep water observations. Thus it is important that a speedy and accurate means be provided for the quantitative analysis of a large number of

records. If the wave record spectrum analyzers mentioned above could be modified so that they will give reliable results, then instead of months per analysis it would require only five or ten minutes to analyze a twenty minute record. It is therefore advisable to analyze a number of records such as the one treated above numerically and then to compare the results with the electronic analysis in order to calibrate the analysis.

Design features of wave record analyzers

The design features of an electronic analyzer will be described in general in order to show what is needed in such an instrument. Plans are being made to modify the instrument devised by Klebba [1946], and a Kay Electric Company sonograph is being studied in order to convert it to a wave analyzer. The above instruments will be modified and interpreted in the light of these considerations.

Wave analyzers should have the following features as suggested by the numerical analysis given above.

1) The length of the record to be analyzed should be of the order of 20 to 35 minutes. Provision for the analysis of variable length records over a range of from 10 to 45 minutes would be advisable but not essential.

2) The band pass filter should be square shouldered and it should have a $\Delta\mu$ proportional to the same value employed in the numerical analysis above. Too wide a band pass would result in poor resolution of swell spectra and too narrow a band pass would result in an extremely erratic analysis. The shape of the filter is very important and the typical tuned circuit response curve is not very good for this application (see Tukey and Hamming [1949] for further details).

Provision for different width filters would be advisable.

3) The band pass filter should not tune through the record too rapidly; that is, the entire record should pass through the filter before it has been tuned through, say, one tenth of its band width.

4) The rectification time constants which provide the output voltage to portray the spectrum should be long enough to average effectively over the entire record.

5) A square law detector would be best so that the graph of the spectrum would be that of a power spectrum.

6) Variable controls should be eliminated, and a choice of four or five calibrated set switch positions provided.

Present results of wave record analyzers

Figure 44 is a collection of examples of electronic analyses as taken from the literature. Various spectra are shown as analyzed by the machines described by Klebba [1946, 1949] and Barber and Ursell [1948]. An autocorrelation as performed by Rudnick's device [1951] is also shown. Some of the spectra have been modified by adding some dashed and dash-dot curves in order to illustrate some points in the forthcoming discussion.

Spectrum number one as shown on the upper left of figure 44 is taken from a paper by Seiwell [1949a]. It is an analysis on Klebba's machine of a pressure record taken in 120 feet of water off Bermuda on 25 October 1946 at 1405 for 350 seconds. For periods less than about 7 seconds the amplitudes are negligible due to the filtering effect of depth.

The dashed curve drawn by eye through the irregular curve of the figure is a smoothed interpretation of what the spectrum might just

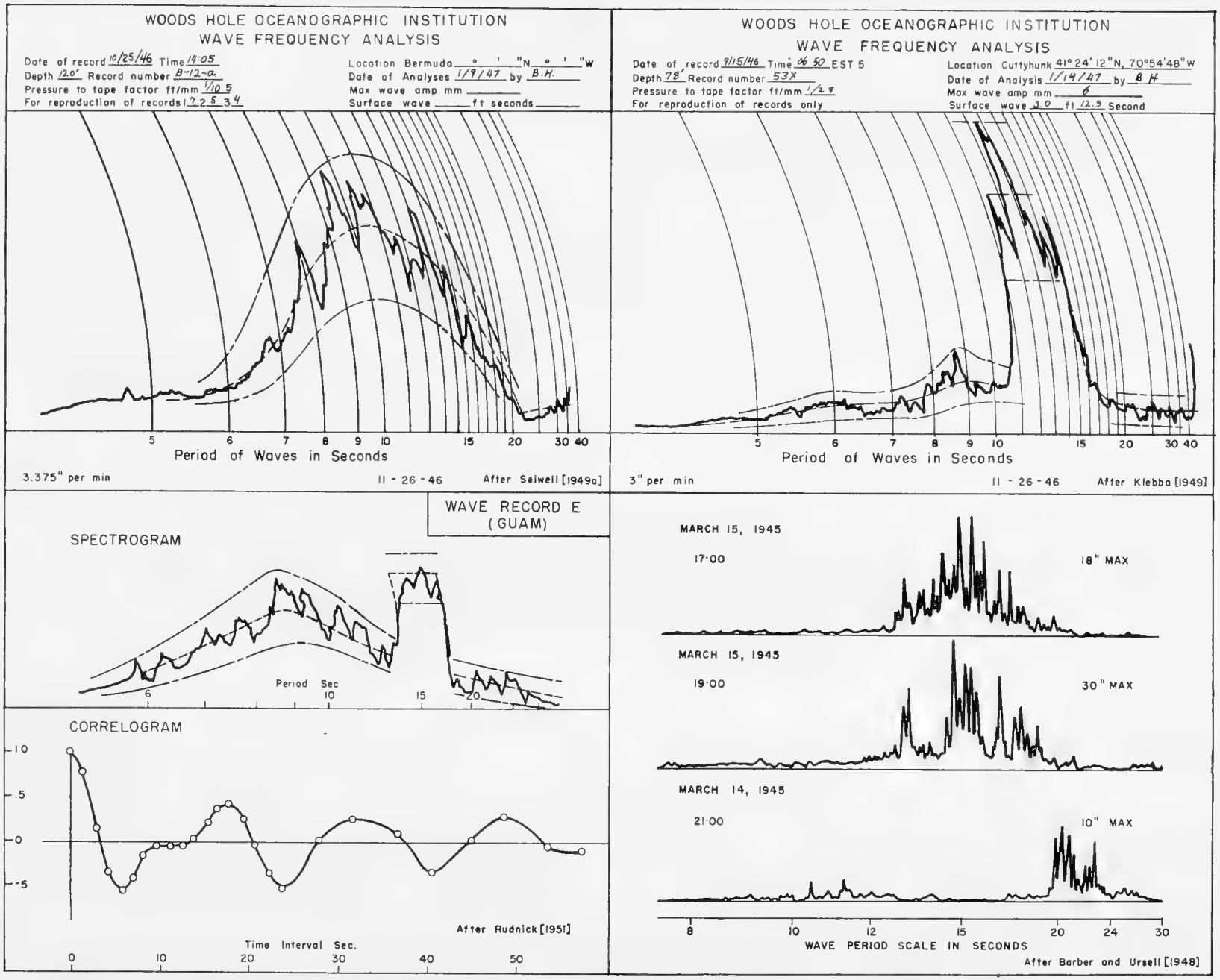

Figure 44. Graphs of various spectra and Autocorrelation Functions obtained by electronic methods.

as well have been given the length of the record and the statistical reliability of the analysis. Stated another way, to prove that the spectrum is actually as irregular as shown a very much longer stationary record would be needed.

The upper and lower dash-dot curves might represent the 90% confidence limits of the analysis, and if the record is related to the square root of the power spectrum then rough computations suggest that the number of degrees of freedom of the analysis lies between 4 and 20 and that it is most likely about 9. Thus the individual peaks and troughs are extremely unreliable.

Nevertheless the analysis shows that there are important contributions to the entire spectrum from μ equal to $2\pi/20$ to μ equal to $2\pi/7$. The record is undoubtedly that of a pressure filtered "sea" record, and the sea surface would best be represented by a spectrum covering a wide band with possibly important contributions even for periods below seven seconds.

Spectrum number two is from the paper by Klebba [1949]. It was taken in 78 feet of water on 15 September 1946 at 0650 EST off Cuttyhunk. Spectral components with a six second period would begin to show in the spectrum if they were present and certainly important ten second components would be evident. They are not present; the highest important value of μ is at $2\pi/11$ and the lowest is at $2\pi/15$. Since the dashed curve could represent the spectrum just as accurately as the one shown, (and since the dash-dot curves again suggest the degrees of freedom of the analysis), it would appear that this record is a clear cut example of a power spectrum such as those predicted in Chapters 7 and 10. The record must have been a "swell" record with a

well defined band width, and the waves must have come from a distant source. Local chop below periods of 6 seconds would be undetectable.

This second spectrum as shown on the upper right of figure 44 is the electronically analyzed spectrum of the classical wave record 53-X. The electronic analysis was first given by Klebba [1949], Seiwell [1949b] gave the same electronic analysis and stated that the analysis "does not permit a reliable interpretation of the physical properties" [of the record].

Seiwell [1949b] then proceeded to interpret the record in terms of a cyclic component of 12.25 seconds and a superimposed series of random fluctuations. His results were debated by Deacon [1951] at the National Bureau of Standards Symposium on Gravity Waves.

Tukey and Hamming analyzed Seiwell's autocorrelation data and the results of the analysis were quoted a few pages back. The power spectrum analysis of the autocorrelation data from record 53-X is given in figure 41. The quotation from Tukey and Hamming and the theoretical results contained in this paper effectively refute the claim of a cyclic component.

Tukey and Hamming were limited at the very start by inadequate data since the original record was too short, the lags were too close together, and there were not enough lags. Their results consequently yielded a spectrum which has practically no resolution over the band of frequencies of importance. From their analysis and from figure 44, it is not too difficult to see how Seiwell might have reached his erroneous conclusions since the swell did have a rather narrow band width. However, the important point is that the electronic analysis in this particular case, when properly interpreted, yields the most nearly correct qualitative spectrum.

Spectrum number three is from a paper by Rudnick [1951].* The record was taken offshore from Guam and additional information on the record can be found in a paper by Miller [1949]. The spectral analysis was made on Klebba's machine. If again the dash and dash-dot curves can be interpreted as before, this record strongly suggests the simultaneous presence of a local "sea" and a "swell" from a distance. The contribution from the "swell" rises significantly above the level of the "sea" record at the same frequencies. As would be expected the correlogram of the record is quite irregular, and it would be difficult to detect the simultaneous sea and swell conditions on the basis of it alone.

The three small spectra on the lower right were taken from the paper by Barber and Ursell [1948]. They were made at Pendeen England on 14 March 1945 at 2100 and on 15 March 1945 at 1700 and 1900. The third spectrum is from swell and the first two spectra are from the same storm after it had moved closer to the coast of England and intensified.

According to Barber and Ursell, the analyzer responds only to certain frequencies which have an integral number of cycles around the wheel on which the record is placed. Barber and Ursell [1948] make the following statement:

> "The record is fastened around the circumference of a wheel which rotates about a horizontal axis carrying the record past an optical system which throws the record a horizontal line of light. The reflected light illuminates light-sensitive cells whose electrical output is, therefore, a continued repetition of the curve on the record. This electrical output is

---

*In this very interesting paper, Rudnick reports that wave records are Gaussian. This important discovery was thus first published by him in 1951. His paper was not known to the author when Part One was published.

amplified and made to drive a vibration galvanometer. It is clear that if there is a component in the record having N complete cycles in the peripheral length of the wheel, this will produce a resonance of the galvanometer at its natural frequency of p cyc./sec. when the wheel is rotating at a speed of p/N rev./sec. The wheel is made to revolve at a speed which gradually decreases from a high value and the vibration galvanometer performs a series of transient resonances, one for each periodicity in the record. The resonances of the vibration galvanometer are converted to an electrical signal which drives a pen recorder, and the curve drawn by this pen is a series of peaks which constitute a Fourier amplitude spectrum on the curve on the record. ...."

The envelope of the individual spikes in the record would seem to be related to the power spectrum of the record. The width and shape of the spike would therefore be related to the band pass filter of the analysis and the figure suggests that the resonant galvanometer is very sharply peaked and responds to an extremely narrow band of the power in the wave record. Note how the amplitude of the record falls down to very low values on each side of each peak.

Now note how extremely irregular the envelope of the peak appears to be. From 1700 to 1900 in the first two spectra marked gaps appear inside of the range of μ where one would expect only minor variations from the theories contained in this paper. If the irregularities were to reflect actual physical changes in the record, this would be most disconcerting, but they really do not.

The irregularities from record to record and from point to point in the same record are simply due to too great a resolution for too small a record length. The wave records were 20 minutes long and there are about 15 spikes between $2\pi/15$ and $2\pi/12$ in the spectra shown. This suggests a band width of the analysis given by $\Delta\mu$ equal to $2\pi/4.15.15$. From equation (10.39), and since 20 minutes times

60 equals 1200 seconds which in turn must equal $N\Delta t$, it follows from equation (10.39) that the analysis has approximately five degrees of freedom.

Table 16 then shows that adjacent peaks can vary by a factor of four above the true value and by a factor of one half below the true value in a power spectrum determined by these conditions.

The spectra shown must probably be squared value for value to get a shape like a power spectrum, and if this is done the variation just described actually occurs.

The resolution employed is very much greater than is needed, and replacement of the galvanometer by a square shouldered band pass circuit about five times as wide as the one employed would be the first step in obtaining quantitative results from this instrument. This would result in twenty-five degrees of freedom and the shape of the spectra obtained would be much more regular. High resolution such as that employed in the above analyzer would require a record five times longer than the one given and very careful design considerations, especially with reference to integration time constants, to yield reliable results.

It would also be interesting for the reader to return to the Appendix to Part One and study the various spectra shown there in the light of these considerations. All the spectra shown, both in the Appendix and in the last figure, show important observational and theoretical properties of the sea surface, but they are not quantitative. They must be made quantitative to provide reliable and useful numerical results.

Conclusions

Power spectra can be computed or determined electronically in a reliable statistical way which will yield valuable information on ocean waves. Two dimensional power spectra are also badly needed, but the one dimensional spectra, such as have been shown, have verified many of the theoretical properties of the sea surface, which were derived in previous chapters. In particular, sea and swell records appear as predicted, and a quantitative spectrum of a pressure record yields correct values for the computation of the properties of the free surface and of the energy flux toward shore.

Acknowledgements

The author again wishes to express his sincere thanks to the many people who have helped in the preparation of this work. The continued help, cooperation, and interest of all of the people and of the organizations mentioned in Part One is deeply appreciated. The interest with which Part One has been received is gratefully acknowledged.

Thanks are also due to Mr. Dean F. Bumpus for the aerial photographs used in Chapter 12. They illustrate many important properties of wave refraction.

July 1, 1952

Willard J. Pierson, Jr.
Department of Meteorology
New York University

Continued Index to the Figures

Continued Index to the Plates

Continued Index to the Tables

Supplementary List of References

Arthur, R. S., [1946]: Refraction of water waves by islands and shoals with circular bottom contours. Trans. A. G. U., v. 27, no. 11.

Davies, T. V., [1951]: The theory of symmetrical gravity waves of finite amplitude. I Proceedings of the Royal Society, A, v. 208, 1951.

Deacon, G. E. R., [1951]: Analysis of sea waves. Symposium on Gravity Waves, National Bureau of Standards.

John, F., [1949]: The action of floating bodies on ocean waves. Annals of the New York Academy of Sciences.

Lee, Y. W., [1949]: Communication applications of correlation analyses. Symposium on Applications of Autocorrelation Analyses to Physical Problems, Woods Hole, Mass., 13-14 June 1939. ONR Dept. of Navy, Washington, D. C.

Luneberg, R. M., [1944]: Mathematical theory of optics. Brown University, summer 1944. (Notes no longer available.)

_____, [1947]: Propagation of electromagnetic waves. Lecture notes, New York University.

Mason, M. A., [1951]: The transformation of waves in shallow water. Coastal Engineering Council on Wave Research. The Engineering Foundation, (pp. 22-32).

Miller, R. L., [1949]: Wave and weather correlation at Apra Harbor, Guam, M. I., from 18 March to 31 May 1949. Wave report from Scripps Institution of Oceanography, No. 90.

Pocinki, L. S., [1950]: The application of conformal transformations to ocean wave refraction problems. Trans. A. G. U., v. 31, no. 6, pp. 856-867.

Rudnick, P., [1951]: Correlograms for Pacific Ocean waves. Proc. of the Second Berkeley Symposium on Mathematical Statistics and Probability. University of California Press, pp. 627-638.

Snodgrass, F. E., [1951]: Wave recorders. Coastal Engineering, published by Council on Wave Research, The Engineering Foundation, pp. 69-81.